University Of Nairobi
College of Architecture and Engineering
Institute of Nuclear Science and Technology

Aerosol impact at high altitude: a case study at 4800 m on Mt. Kenya

by:

Anne Wambui Mutahi

S56/61776/2013

BSc Environmental and Biosystems Engineering

A thesis submitted in partial fulfilment for the degree of Master of Science in Nuclear Science in the Institute of Nuclear Science & Technology in the University of Nairobi.

@October 2016

Declaration

This thesis is my original work and has not been presented for a degree in any other university.

Sign …… Date ……..

Anne Wambui Mutahi
S56/61776/2013

Supervisors' approval

This thesis has been submitted for examination with our knowledge as university supervisors.

Professor M. J. Gatari
Institute of Nuclear Science and Technology
University of Nairobi

Sign …….....……..
Date …….....…….....

Professor Johan Boman
Department of chemistry and molecular biology
University of Gothenburg

Sign …….....……
Date.….....……

Dr. August Andersson
Department of Applied Environmental Science
Stockholm University, Sweden

Sign …….....……...
Date …….....…….

Dedication

I dedicate this thesis to my beloved husband Josphat and son Tavian and my entire family for supporting me all through.

Acknowledgments

As I pursued accomplishments in the academics, I am really grateful for the assistance, leadership and love that I have been given in the course of completing my study.

First and foremost, I would like to thank God the Almighty for being healthy, strong and protected throughout the period of my study.

I want to recognize and thank Professor M. J. Gatari who co- originated this research project and his devoted contributions towards this work through invaluable support and guidance in the duration of this project. I would additionally wish to appreciate Professor J. Boman and Dr. A. Andersson, my other supervisors, for their very helpful input, advice and confidence in me.

I am also thankful to Kenya Nuclear Board for offering me a scholarship and also the International Science Programme for funding this study.

I am also grateful to the Director Institute of Nuclear Science and Technology Mr. Maina D.M, Mr. Simion Bartilol, Patrick Kamau, Mathias Mailu, Daniel Njoroge and Charles Gachara of the Institute of Nuclear Science and Technology, whose assistance were really significant during the collection and analysis of samples.

I would also want to thank the Kenya wildlife service especially Dr. Thadeus O. Obari, chief Warden Mt. Kenya National park Simon Gitau and the rangers for their support during my sampling period.

Table of Contents

List of Tables

List of Figures

List of Abbreviations and Chemical Symbols

ADD	Aerodynamic Diameter
ASL	Above Sea Level
BC	Black Carbon
CH_4	Methane
CNN	cloud condensation nuclei
CO	Carbon Monoxide
CO_2	Carbon Dioxide
EDXRF	Energy Dispersive X-ray Fluorescence
GHG	Green House Gases
HKH	Hindi-Kush-Himalaya
IN	ice Nuclei
IPCC	Intergovernmental Panel on Climate Change
N_2O	Nitrous Oxide
NO_X	Nitrogen Oxides
PCA	Principal Component Analyses
PM	Particulate Matter
RH	Relative Humidity
SHARE	Stations at High Altitude for Research on the Environment
STP	Standard Temperature and Pressure
SO_2	Sulphur Dioxide
TVOCs	Total Volatile Organic Compounds
TXRF	Total Reflection X-ray Fluorescence

Abstract

One of the biggest challenges of the 21st century is climate change. It has been characterized by a rise of the mean temperatures of the ocean and air, thinning of glaciers and snow cover as well as rise in sea level. It has also been linked to extreme global weather conditions. Among the causes of climate change is elevation in the amounts of atmospheric aerosols and greenhouse gases, mainly as a result of anthropogenic activities. In order to quantify and mitigate these effects, it is important to have adequate observational aerosol data, from which; formation, chemical composition and transformations of the aerosols and trends can be obtained. Therefore, this study was aimed at understanding major air pollutants at high altitude, the need to improve understanding on aerosol sources and impact on glacial melting and the degradation of mountain ecosystems. A sampling campaign for the study was carried out on Mt Kenya, the second highest mountain in Africa, from 2nd to 7th March 2015 and sampling done for 8 hours daily at sampling periods of 8 h per day for five days and two nights.

Instruments used for sampling were BGI 400S for $PM_{2.5}$, MicroAeth Model AE51 for BC and GrayWolf pack for gases and particle counting. Quality control on EDXRF spectrometer was done using SRM 2783; Sensitivity, intensity and resolution were confirmed on TXRF spectrometer. Filter analysis was done using EDXRF spectrometer and glacier analysis in the TXRF spectrometer and the quantitative elemental analysis were done using AXIL and S2 Picofox software respectively. Basic and Multivariate, Principal Component analysis (PCA), statistics were used for data analysis.

$PM_{2.5}$ concentration reported a range of 10 - 207 ng m^{-3} with elemental composition dominated by Ca and Fe with concentration ranges of 5854 - 26626 ng m^{-3} and 96 - 855 ng m^{-3} respectively. Daily BC mean concentration ranged between 123 - 263 ng m^{-3}. Atmospheric gas that were significantly high throughout the study was CO_2, which implied high oxidation of their precursors, CO. This was observed as the reason why there was no O_3. In the dirty glacier; K, Ca, Ti, V, Mn, Fe, Cu and Br were higher than in the clean glacier samples. However, Cr and Ni remained equal in both glacier. The PCA analysis results of elemental concentrations gave two components showing PM2.5 particles were mainly

from mineral dust and industrial sources. However, the industrial source was weaker than the mineral dust implying a strong impact of dust at the measurement site. The observations in this study, implicated impact of long and short range transport which one would expect in the middle troposphere. However, further short term studies and spaced in time over the year are recommended. The best alternative to spaced short term studies is installation of an automatic sampling site, which could be supported by validated by random
short term studies.

CHAPTER ONE

1.1 Introduction

Extreme weather conditions have in the recent past marked the global climate variability, spanning from the north to the southern hemispheres. The frequency of occurrence of these severe weather events have been on the rise, and they include the most recent typhoons in Philippines, floods in Rio de Janeiro, extreme winter in America, and the persistence drought in Eastern and Southern region of Africa. These are just a few and they are becoming severe over time (BBC, 2015). There is also concern on the rapid melting of the glaciers on the mountaintops, implying warming at high altitudes. According to Intergovernmental Panel on Climate Change (IPCC, 2007), aerosols are key contributors to climate change, and the biggest source of uncertainty in future climate predictions. Besides impact on climate change, atmospheric aerosols affect visibility, health, atmospheric chemistry and biogeochemical cycles in different ecosystems, the hydrological cycle, the earth's radiation balance, as well as levels of greenhouse and reactive trace gases (Gatari et al., 2009; Ramanathan & Carmichael, 2008; Poschl, 2005).

An aerosol is defined as the liquid or solid particle suspended in air/gas (Hinds, 1999) including the suspending gas. The particulate component of the aerosol range in size from a few nanometers to micrometers, and are associated with phenomena such as dust, haze, smoke, mist, fog, smog and fume (Seinfeld and Pandis, 1998). The principal chemical constituents include sulfates, ammonium, nitrates, mineral dust, sea salt, elemental or black carbon, and organic compounds, originating from various natural or/ and anthropogenic sources (Poschl, 2005). The human inhalable aerosol particle size range is categorized into two groups; fine size range has particles of aerodynamic diameter (ADD) of $< 2.5\mu m$ and coarse range has of $2.5 \leq ADD < 10\ \mu m$. The former is also of great importance in climate change for it has long life times in the atmosphere and contains most of the black carbon particles, which are efficient absorbers of solar radiations.

Atmospheric aerosol has a strong influence on the transfer of radiant energy, as well as the spatial distribution of latent heat in the atmosphere, consequently having an influence on weather and climate. For instance, aerosol particles act as condensation nuclei, which is essential in formation of clouds and ice crystals. In addition, aerosols play an essential role in cooling or warming the atmosphere, by either scattering or absorbing solar radiation. For example, some aerosol components like mineral dust and black carbon absorbs the incoming solar radiation and retains the outgoing terrestrial radiation on the earth's surface through different mechanisms (Twomey, 1977; Haywood & Boucher., 2000; Andreae, 1990).

Black carbon is the black component of atmospheric PM, which is emitted from incomplete combustion process of fossil fuels, biomass and biofuel (Masiello, 2004). One of the distinctive characteristics of Black Carbon (BC) is its large mass absorption efficiency. It absorbs high solar energy per unit mass in the atmosphere, and can absorb a million times more energy than CO_2 (Bond and Sun, 2005). Therefore, the accumulation of black carbon in the atmosphere, and more specifically in the mountaintops, causes the darkening of snow and ice surfaces. The darkened surfaces decreases solar radiation reflectivity (albedo), and increases heat absorption, thus accelerating glacial and ice melting. This makes BC a significant climate warming pollutant in regions of the world affected by combustion emissions.

Mineral dust is a crucial aerosol to take into account in relation to climate change, due to the fact that its anthropogenic and natural sources account for 30 % to 50 % of the overall aerosol emissions by mass (Bian and Zender, 2003). Some of these sources include wind erosion, soil re-suspension, some agricultural practices and industrial activities (IPCC, 2013). Mineral dust plays a role in reduction of the intensity of solar radiations reaching the earth's surface through absorption and scattering as it enters the atmosphere. Its deposition on snow reduces the ability of the snow to reflect solar radiation, and nearly doubles the amount of heat absorbed causing a fast melt (Bian et al., 2003).

Atmospheric aerosol particles may either be emitted directly into the atmosphere, or as secondary particles through oxidation of precursor gases e.g. NO_X, SO_2, and VOCs.

Therefore, influence of these gases on climate should not be underestimated. For example, the sulphate component is the largest single contributor to aerosol cooling effect (Jacobson, 2001). On the other hand, greenhouse gases like CH_4, N_2O and CO_2, have been associated with the rising global temperatures.

Understanding the actual composition and concentrations of atmospheric aerosols is critical in determining their sources, as well as predicting their impact on various atmospheric processes. This calls for numerous relevant studies to be conducted around the globe However, contributions from Africa have been minimal and this motivated interest of carrying out this study.

1.2 Problem Statement

One of the biggest challenges of the 21st century is climate change. The warming of the climate system is incontrovertible, as characterized by increasing global Mean Ocean and air temperatures, thinning of glaciers and snow cover, and rise in sea level. These effects have been attributed to elevated concentration of atmospheric aerosol and greenhouse gases mainly due to anthropogenic activities. In order to quantify and mitigate these effects, it is important to have adequate observational climate data, from which aerosol particle formation, chemical composition and transformations and trends can be obtained. However, available data is not sufficient, and there is a notable lack of geographic balance in data and literature on observed changes, with marked scarcity in developing countries (IPCC., 2007). For example, Gatari et al., (2009), observed that there is lack of sufficient knowledge and understanding of pollutants and their sources, within the African continent compared to other parts of the world. Studies carried out at Stations at High Altitude for Research on the Environment (SHARE) in Nepal, Italy and Pakistan have contributed to the limited knowledge of particulate matter and black carbon (Lau et al., 2010). Within the African continent particularly equatorial Africa similar studies were conducted on the northwestern slopes of Mt. Kenya (Henne et al., 2008; Gatari et al., 2009) at 3678 m above sea level (ASL) in central Kenya, and at 4760 m on Mount Rwenzori (Lentini et al., 2011) in West Uganda. The studies recommended more studies of the aerosol at high altitude to

improve understanding of the impact of increasing emissions from human activities in the perspective of climate change in equatorial Africa.

Currently, the available data from high altitudes is insufficient besides lack of geographic balance in observations with marked scarcity in developing countries, especially in mountains. The mountains are mostly seen as being areas of "clean" environment due to their inaccessibility to human population.

This study was, therefore, planned to evaluate the aerosol impact at a higher altitude than that of Gatari et al. (2009) and Henne et al. (2008), but on the western slopes of Mt. Kenya.

1.3 Objectives

The main objective was to determine the concentrations of aerosol species at a high altitude site on Mt Kenya and to assess their possible sources.

The specific objectives of the study were;

1. To sample and analyze qualitatively and quantitatively the aerosol $PM_{2.5}$ and glacier at a high altitude site on Mt Kenya.
2. To determine atmospheric concentration of black carbon in the sampled $PM_{2.5}$.
3. To sample and analyze atmospheric SO_2, $NO_{X,}$ TVOC, CO_2, O_3 and CO together with relative humidity, temperature, wind direction and speed.
4. To assess possible sources of the observed aerosol species.

1.4 Justification and Significance

Through this study, information on various properties of the atmospheric aerosol such as elemental content in PM2.5 and glacier, and concentrations of black carbon and gaseous species will be evaluated. This will play a critical role in bridging the knowledge gap of the aerosol at high altitude in Tropical Africa. It will also contribute additional information that can be exploited for climate change policy formulation and mitigation strategies by governments and other stakeholders thus, helping in making well founded decisions to improve the current situation. In addition, the study will set a base for further research

focusing on impacts of the aerosol at high altitude on Mt. Kenya and assessment of consequences to sustainable economic development in the country besides use for regional and global climate change studies.

CHAPTER TWO

LITERATURE REVIEW

2.0 Introduction

This chapter will investigate different types and sources of aerosols, and how they impact at high altitude regions in different ways as discussed by various authors in their research work. The reviewed information will help to provide detailed knowledge on atmospheric aerosols mined through some of the previous studies.

2.1 Role of Atmospheric Aerosols

Aerosols play an essential role in the overall energy balance of the atmosphere. This is through direct effects such as absorption and scattering of outgoing and incoming terrestrial and solar radiation, and indirectly through modification of microphysical properties and size of clouds, through their role as cloud condensation nuclei (Marcq et al., 2010). Aerosols also provide sites on which chemical reactions take place. For instance, the tendency of aerosols to catalyze the chlorine gas and nitrogen reaction in the stratosphere is a prime contributor to stratospheric ozone destruction (NASA, 1996).

2.1.1 Aerosol Types

Aerosols are ever-present in the atmosphere, in a wide range of concentration levels and distribution in space and time. They are generally heterogeneous. They vary in size, shape, source, chemical composition and life times. It is therefore important to classify aerosols into different categories. However, there is no particular format that can be used to fully and systematically categorize the aerosols. Various parameters such as origin, size, formation, chemical composition, geographical location, among others, can be used. Here is a brief description of various classifications used to describe aerosols.

Based on their origin, aerosols are generally categorized as either natural or anthropogenic. Natural aerosols comprise of emissions from soils, ocean, vegetation, volcanoes and forest fires. On the other hand, anthropogenic aerosols are predominantly the emissions from combustion of bio-fuels, fossil fuels, among other forms of fuels, industrial activities,

transportation and domestic activities. Using principal component analysis (PCA), it is possible to distinguish between natural and anthropogenic aerosols (Shaltout et al., 2013).

Aerosols can further be categorized as either primary or secondary aerosols. Primary aerosols are particulates released in their initial form directly into the atmosphere, whilst secondary aerosols refer to particulates formed through gas - particle conversion processes in the atmosphere e.g. sulfates, nitrates and some organic compounds. Chemical composition can be used to distinguish between these two types. Aerosols can also be classified based on their geographical location and properties using terms such as urban aerosols, marine aerosols, desert dust, continental aerosols, biogenic aerosols, volcanic aerosols or stratospheric aerosols. However, aerosols can be transported over long distances to different locations.

Chemical compositions of aerosols are highly diverse. Based on chemical component, aerosols can fall under five main categories; sulfates, nitrates, carbonaceous aerosols (black carbon and organic carbon), sea salt and mineral dust (Ramanathan, et al., 2001).

2.1.2 Aerosol Sources

Mountain tops are usually regarded as 'clean regions', however, they are also strongly impacted by pollution from anthropogenic sources. (Henne et al., 2004). In most developing countries like India and Kenya, anthropogenic pollution is the primary source of high altitude aerosols. A study done on southern parts of the Himalayas suggested that typical valley circulations uplift significant amounts of pollutants which are diverted by long range and regional transport events (Bonasoni et al., 2008, 2010). According to Yasunari et al. (2010), high altitude studies give us an opportunity to monitor the effects associated with anthropogenic pollutants transported to such remote regions. In order to determine the proper mitigation measures of emission of $PM_{2.5}$ from anthropogenic activities, there is need to know the stationary and mobile sources(Wada et al.,2016)

Natural sources of great importance include: eruptions of Volcanoes that eject huge columns of ash, sulfur dioxide and other gases into the atmosphere; Forest fires that release partly burned organic and black carbon into the air; and lastly, certain plants varieties that

release gases, which in turn react with other chemical components in the air to yield secondary aerosols. For example, there are various kinds of microalgae thriving in the ocean that release sulfurous gas (dimethylsulfide), which is converted into sulfates in the atmosphere. However, dust and Sea salt are some of the most prevalent PM in the atmosphere. They are mainly as a result of sandstorms that blow tiny pieces of mineral dust into atmosphere from deserts, and wind-blown sprays from the ocean waves that flings sea salt aloft (Kahn et al., 2010). There are Anthropogenic and natural sources of BC but mainly Incomplete combustion of fossils fuels is the main source(Ogren and Charlson,1983;Akhter et al,1985; Cai et al 2014).

Anthropogenic activities that contribute to aerosols in the atmosphere include;

- combustion of fossil fuel producing huge volumes of SO_2, which reacts with other gases and water vapor in the atmosphere to form sulfates.
- Biomass burning, which is one of the commonly used method for clearing land and reducing farm waste. It produces smoke that is composed mainly of black and organic carbon.
- Incinerators, automobiles, power plants and smelters, are prolific producers of black carbon, nitrates, sulfates, among other particles.
- Overgrazing, drought, deforestation and excessive irrigation, can modify the soil properties thus escalating the rate at which dust particles enter the atmosphere.
- Indoors, common sources of aerosols are cooking stoves, cigarettes, candles, fireplaces and lamps (Kahn et al., 2010).

According to Voiland (2010), aerosol particles are present throughout the atmosphere; air over oceans, mountains, deserts, ice, forests etc., and irrespective of their minute sizes, they have considerable effects on climate. The main aerosol types are black carbon, sulfates, nitrates, organic carbon, sea salt and mineral dust. These particles often clump together to form complex mixtures. Satellite monitoring and In situ observations have evidently shown the existence of polluted tropospheric layer (Bonasoni et al., 2010; Ramanathan et al., 2007). For example, investigations by Ramanathan et al. (2007) showed a brown cloud (regional

scale plume of air pollution made up of massive amounts of aerosols e.g. fly ash, soot, nitrates, sulfates, and other pollutants) of a vertical thickness of 3km stretching from the Indian Ocean to Himalaya ranges, especially during the dry seasons.

2.2 Impacts of aerosols on high altitude regions.

Aerosols can be transferred over very long distances to remote and "clean" background areas such as high altitude regions, with substantial effect on regional climate. This is common during dry seasons due to the absence of precipitation hence the slow rate of removal from the atmosphere. Marcq et al. (2010) associated heating of the lower atmosphere at levels above the IPCC estimates for GHG related warming, in high altitude regions of Himalayas, to particulate matter transported from both regional and long range distance. According to the author, this observation would influence the local energy balance in two ways. First, it leads to increase in surface temperatures due to presence of absorbing particles, which causes an increase in snowpack melting rate. Secondly, there is a substantial reduction in the intensity of solar radiations reaching the earth's surface, resulting in a decline in surface temperatures. These two observations have a reverse effect on each other, thus limiting the melting rate.

Particulate matter and black carbon exhibits both seasonal and diurnal variations in concentration levels (Marinoni et al., 2010; Marcq et al., 2010). A study conducted in a high altitude research station (5079 m A.S.L) by Marinoni et al. (2010), recorded the highest aerosol concentrations during daytime as well as in pre-monsoon season. The pre-monsoon maxima were associated with increase in anthropogenic activities as well as dry weather conditions, while daytime maxima were attributed to upvalley thermal winds. More studies of aerosols on remote regions to establish the emission sources, assess long range transport, as well as validate global and regional models were recommended.

A study on black carbon (BC) in Asia at high altitude region, by Ming et al. (2013), showed that distribution of BC deposition on the surfaces of high altitude Asia-glaciers largely varied according to elevation (the lower sites recorded higher concentrations and vice

versa), surface melting conditions and regional emission intensities. In addition, BC levels on these glaciers were found to be similar to those recorded in other remote areas, for example in the western American mountains and the Arctic, but considerably less than heavily industrialized regions like northern China.

On Mt. Ruwenzori, large-scale atmospheric air circulation is highly contributed by Equatorial Indian Ocean circulations with an occurrence of 23.3 %. The contribution occurrence from the Arabian Peninsula is 15.9%, regional 16.9%, North Indian Ocean 16.4 % and south Indian Ocean 15.0%. The circulation occurrences from the different regions are likely to influence the mountain atmospheric aerosol properties due to stratospheric air intrusion, transport of biomass burning emissions and mineral dust (Lentini et al, 2011).

Aerosol transportation from different sources is also evident on Mt. Kenya. Gatari et al. (2008) argued that comparable levels of mineral dust, sulfate and BC were not only influenced by anthropogenic activities in the region near the mountain and southeastern Kenya, especially from the cities of Mombasa and Nairobi, but also ocean traffic from the Indian Ocean and others outside the East African coast.

2.2.1 The Earth's radiation balance

Atmospheric aerosols play a crucial role in the earth's radiative balance, either through direct effects such as absorption and scattering of radiations, or indirectly through modification of microphysical properties of clouds through cloud condensation nuclei (CCN) and ice Nuclei (IN) (Yu et al., 2006; Marcq et al., 2010). Therefore, addition of aerosols in atmosphere may result in a net positive or negative change in radiative fluxes. A net positive radiative warming effect signifies that energy has been added to the earth-atmosphere system, whereas a net negative/ cooling effect signifies that there is an overall loss of energy.

It is estimated that the degree of direct radiative effects as a result of BC is 14% more than that of methane in the marine boundary layer (Jacobson, 2001). Horvath (1993) pointed out that in the visible spectrum, BC is the most effective light absorbing aerosol species, and hence it greatly contributes to climate change. Moreover, aerosols radiative forcing is

dependent either directly or indirectly upon various characteristics of the particulates involved, such as existence of absorbing materials, mass concentration as well as size distribution (Marinoni et al., 2010).

Absorbing aerosols for example BC and mineral dust, and to some extent the brown clouds effectively absorbs solar radiations, enhancing the atmospheric warming (Bond and Sun, 2005). Consequently, this contributes to global warming, particularly in areas where anthropogenic emissions are high. According to IPCC (2007), BC was accountable for global warming by approximately 0.5 Wm^{-2} compared to methane, which is second most significant compound in global warming after CO_2.

In high altitude areas of Hindi-Kush-Himalaya (HKH), absorbing aerosols were found to heat the mid troposphere through absorption of solar radiations (Lau et al., 2010). This heating process produces an atmospheric dynamical feedback, called Elevated-Heat-Pump (EHP) effect, resulting in increased precipitation in India. Therefore, it is evident that the amount of radiation received at the surface is clearly modified by the presence of aerosols even at high elevation (Ming et al., 2013).

Absorbing aerosols in elevated regions of Hindi-Kush-Himalaya (HKH), heat the mid troposphere by absorbing solar radiation (Lau et al., 2010). This heating process produces an atmospheric dynamical feedback, referred to as Elevated-Heat-Pump (EHP) effect, resulting in increased precipitation in India. Therefore, it is evident that the amount of radiation reaching the earth's surface is definitely modified by aerosols present even at higher altitude (Ming et al., 2013).

2.2.2 Glaciers

Deposition of aerosols on glaciers increases the rate of snow and ice surface warming, which consequently accelerates the rate of glacier melting, shortens snow cover period, as well as modify the mass balance, hence triggering retreat of the glacier (Yasunari et al., 2010). All these physical activities influence the volume of water available in the area (Flanner et al., 2007; IPCC, 2007). For instance, as these glaciers recede and discharge its stored water, water-flow increases temporarily, however, the future fresh water supply is

threatened (Yao et al., 2004; Kehrwald et al., 2008). Therefore, the probable end result of glacier loss will be heavier spring floods and much reduced fresh water availability during subsequent dry seasons (Xu et al., 2009).

The IPCC (2007) report estimated that global mean radiative forcing caused by BC in snow and ice at $+0.1 Wm^{-2}$, where the discrepancy between different regions was very significant due to their emitting intensities, topography, regional atmospheric circulations, ocean-land distributions, among other factors. The report further acknowledged a low level of scientific understanding regarding this effect. According to Flanner et al. (2007), an addition of 500 ppb of black carbon onto snow decreases its visible albedo from 0.98 to 0.88, and in some places snow darkening is an important component of climate forcing by carbon aerosol. This in turn affects snow melt, duration of snow cover and water flow.

Glacier recession trends have been a major concern in the past century. In East Africa, effects are evident on Mt. Kenya and Mt. Kilimanjaro, where the glacier surface reduced by 75 % and 85 % respectively in the 20^{th} century (Kaser et al., 2006). In the same region, Elena Glacier on Mt. Rwenzori reduced by 60% (Kaser, 1999), resulting in rise in water levels of Lake Victoria by upto 2.5m (Kite., 1982; Lentini et al., 2011). The main driving force of the retreat is the increase of air temperature (Taylor et al., 2006), and incoming short wave radiation with drier atmosphere in East Africa (Molg et al., 2006).

A study on the largest glacier on Mt. Kenya, Lewis Glacier (GRID-arenda,.2007) reported a reduction of that glacier from approximately 1500 m in length in 1900 to less than 750 m in 2004 as indicated figure 2.1.

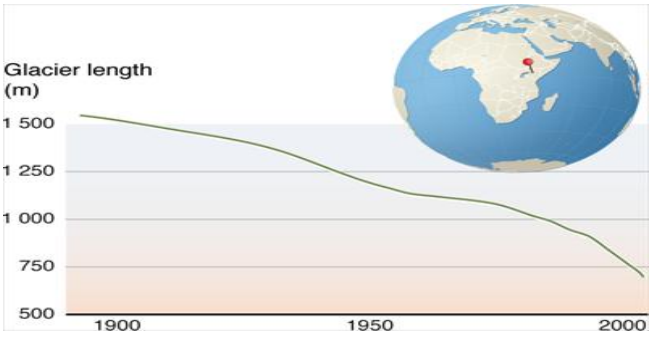

Figure 2.1: Shrinking Lewis Glacier, Mount Kenya (GRID-arenda,.2007)

CHAPTER THREE

MATERIALS AND METHODS

3.1 Introduction

This chapter outlines the steps that were used to gather relevant data useful in bridging the identified research gap. It includes sampling location, sampling procedures and instruments, quality control, elemental analysis and data analysis.

3.2 Sampling Location

This study was carried out on Mt. Kenya, which is the second highest mountain in Africa after Mt. Kilimanjaro. The site was at an altitude of about 4800 m ASL, in Mt. Kenya National Park near the base camp area of the Austrian Hut, western side of the mountain (Figure 1). The area is characterized by tropical alpine highland glacier, and subdivided by three distinctive peaks: Batian, 5199 m ASL; Nelion, 5188 m; and Lenana, 4985 m. There are also lower peaks and lakes: Lakes Ellis, Alice and Michaelson, which play a major role as water source of various rivers. Mt. Kenya is astride the equator at 37.1° E. Its ecosystem supports a large population in Kenya by virtual of being a major water catchment area. For example, River Tana whose main source is Mt. Kenya has five hydroelectric power stations and supports a large population of human beings and animals in Kenya. Consequently, perturbation of the Mt. Kenya ecosystem is detrimental to sustainable economic development and food security in Kenya.

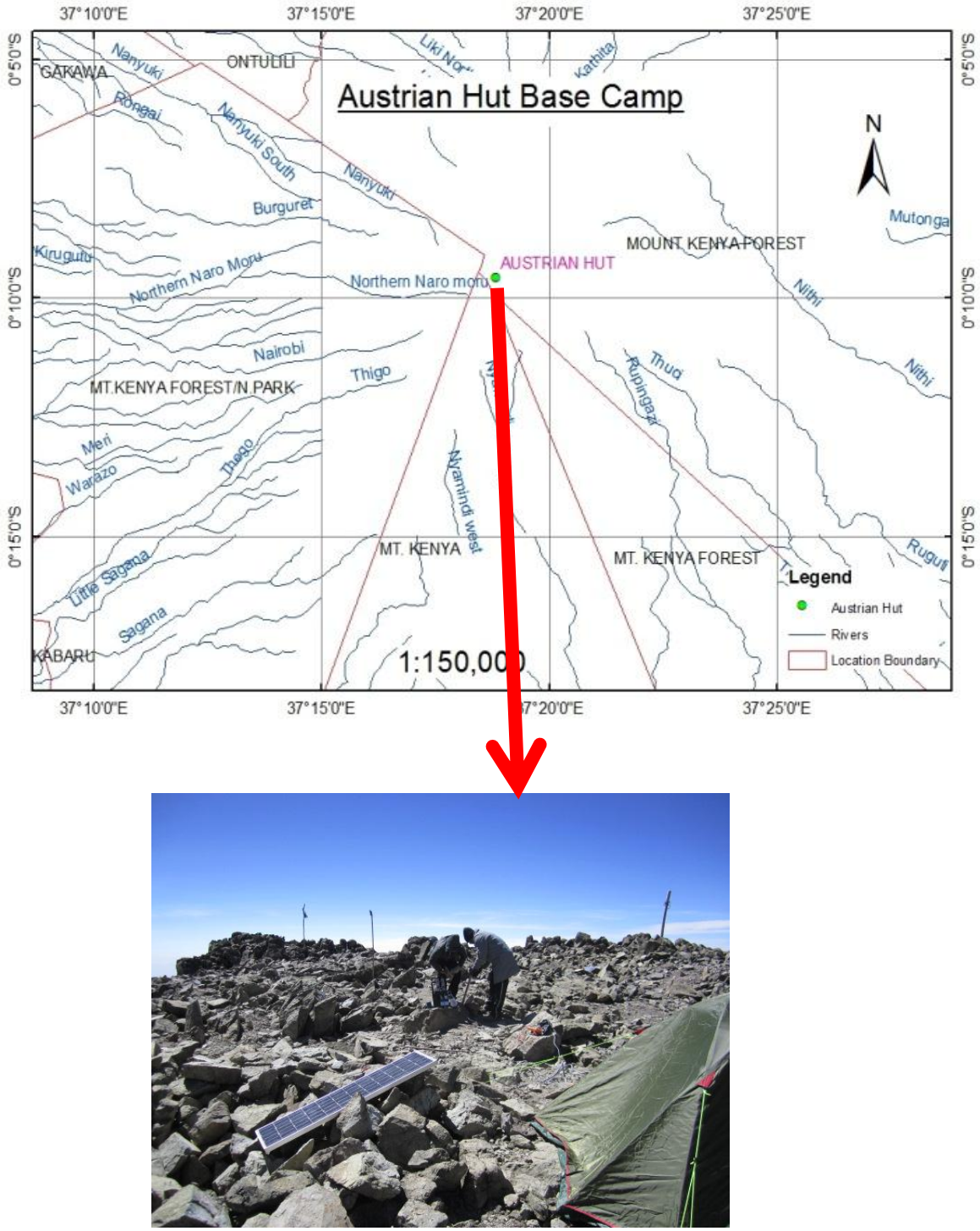

Figure 3.0.1: Map and the sampling site on Mount Kenya.

3.3 Instruments and Sampling

To achieve the objectives of this study, the following instruments were used for sampling: personal samplers, BGI 400S for $PM_{2.5}$; MicroAeth Model AE51 for black carbon monitoring; and GrayWolf pack for gas species monitoring and a particle counter.

3.3.1 Particulate Matter, $PM_{2.5}$

Fine particulate matter ($PM_{2.5}$) were sampled using personal samplers, BGI 400S .It is a cyclone sampler with a geometry that allows only $PM_{2.5}$ particles to be deposited on a filter media (PallRJP2037). Clean Teflon filters, 37 mm in diameter and a pore size of 2 μm were loaded on the filter holder. The sampler used a rechargeable battery that run for long 8 h, thus making it convenient for $PM_{2.5}$ study at remote sites.

Pre-weighed filters were loaded into a cassette, which was then connected into the nozzle, and placed in a sampling position. Samples were collected for 8 h for two days hence sampling for 16 hours, after which the filter cassettes were offloaded and sealed carefully in air tight petri dishes and enclosed in a clean environment to avoid contamination. The flow rate was measured when the clean filter was loaded and at the end of sampling using a field rotameter. The rotameter was calibrated at 4 different flow rates in the laboratory using a flow meter to facilitate a calibration graph for use in establishing correct average sample flow after the field campaign. The sampler's battery was charged using an external battery connected to a solar panel.

In the laboratory, the sample filters were weighed and the difference in weight between it and empty was calculated to obtain the mass of the particulate matter. The concentration of the particulate matter was obtained by dividing the mass of the particulates by the volume of sampled air (equation 3.1).

$$\text{Concentration } (\mu gm^{-3}) = \frac{Wf - Wi}{V} \quad \text{..... Equation 3.1}$$

where;

W_f is the average weight of the loaded filter in μg

W_i is the weight of the unloaded filter μg

V is the volume of sampled air in m^3.

3.3.2 Black Carbon

The black carbon (BC) was measured using AethLabs microAeth, Model AE51, BC monitor shown in figure 3.2. It is a portable and highly sensitive instrument with an Internal rechargeable lithium-ion battery. It is designed for real time measurement of the optically-absorbing BC component of aerosol particles. It drew in air at a flow rate of 150 mL min^{-1} through a 3 mm diameter portion of a filter media. Optical transmission of a stabilized 880 nm LED light through the sample spot is measured by a two photodiode detectors. A filter strip containing T60 Teflon-coated borosilicate glass fiber filter material was changed in every sampling period. The absorbance of the spot was measured relative to an adjacent reference portion of the filter once per time-base period. A study by Cai et al. (2014) reported high reproducibility of results on the fixed site monitoring with a relative standard deviation of 8 ± 5%.

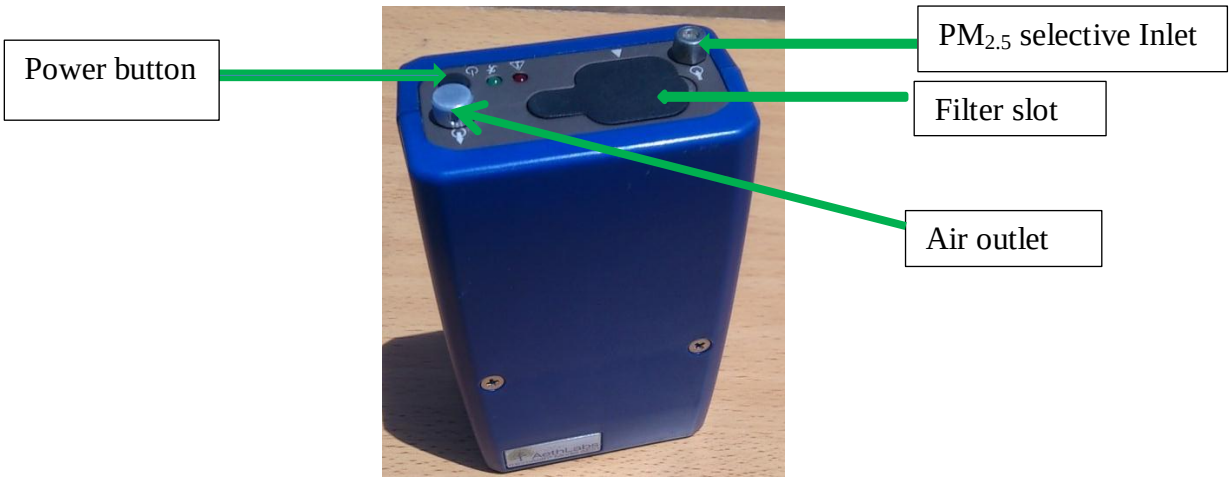

Figure3.2: AethLabs microAeth BC Monitor, Model AE51

The monitor was run for a period of eight hours per day throughout the sampling period. The instrument firmware uses known absorbance per unit mass of BC and flow rate data to calculate the BC concentration in ng m^{-3}.

3.3.3 Glacier and water analysis

Sampling of the glacier was done in three parts namely, dirty glacier, clean glacier and glacier runoff. Dirty glacier was collected from the top layer of the glacier mass. For the clean glacier, 10 cm of the top glacier was removed then the glacier was sampled. The runoff was sampled at the edge of the glacier where the melted water was running down from the glacier.

The whole procedure is illustrated in figure 3.3 and the samples were collected in pre-cleaned plastic bags for laboratory analysis.

Figure 3.3: Figure illustrating the sampling of (a) Dirty Glacier, (b) Clean Glacier, (c) Glacier runoff and (d) collected sample

3.3.4 Atmospheric Gases

Atmospheric gases; SO_2, NO, NH_4, NO_2, NH_4, H_2S, TVOC, CO_2, CO and O_3 concentrations, temperature and relative humidity were measured using GrayWolf Pack (GrayWolf Sensing Solutions) gas measurement instrument shown in Figure 3.4. This instrument was factory calibrated and was on its first use at a high altitude in Kenya.

Figure 3.4: GrayWolf Atmospheric gas monitoring instrument (GrayWolf Sensing Solutions)

The pack had two probes, model TG 501 and IQ 610, which have sensors for specific gaseous species (Table 3.1). Probe TG501 measures SO_2, NO, NH_4, NO_2 and H_2S, and probe IQ 610 ; TVOC, CO_2, CO, O_3 (Concentrations were set in µg m^{-3}), relative humidity (%RH) while temperature (ºC) is measured in both probes. The sensors generate electrical signals which magnitudes are proportional to the amount of the sensed gas species. The signals are amplified, digitized and firmware transformed to concentrations and stored as per the setting. After the field measurements the concentrations were downloaded to the laptop for further analysis using statistical methods.

Table 3.0.1: Sensors specifications in the Graywolf Pack instrument (GrayWolf Sensing Solutions)

Measured parameter	Sensor Type	Range	Accuracy or Lower Detection Limit
Temperature	Platinum resistance thermometer	-10° to 160°F (-25° to +70°C)	±0.3°C
Relative Humidity	Capacitive	0 to 100%RH	±2%RH <80%RH ±3%RH>80%RH
Carbon Dioxide	Non dispersive Infrared	0 to 10,000ppm	±3%rdg ±50ppm
Carbon Monoxide	Electrochemical	0 to 500ppm	±2ppm <50ppm, ±3%rdg >50ppm
VOCs	photoionization detectors	5 to 20,000ppb	Resolution 1ppb, L.O.D. <5ppb
Ammonia	Electrochemical Standard range sensor High range sensor	0.0 to 100.0 0 to 1000	L.O.D <1.0 ppm L.O.D 12 ppm
Hydrogen Sulfide	Electrochemical	0.00 to 50	L.O.D <0.03ppm
Nitrogen Dioxide	Electrochemical	0.00 to 20.00	L.O.D 0.02ppm
Nitric Oxide	Electrochemical	0.0 to 250.0	L.O.D 0.2ppm

3.4.5 PM_{10} Particle counter.

The counter uses optical methods for particle counting and has cyclones that select particle size that enters a specified channel, at a flow rate of 2.8 LPM. The channels select particles sizes (d_p) of a given range of ADD and they are: $d_p < 0.3$ µm; $0.3 \leq d_p < 0.5$; $0.5 \leq d_p < 1.0$; $1.0 \leq d_p < 2.5$; $2.5 \leq d_p < 5.0$; $5.0 \leq d_p < 10$; and for total count (TPM) $d_p > 10$. The counted number of particles was logged in the instrument at every 5 minutes including the counting volume of air in µg m^{-3}. Density of carbon is assumed = 2.5 g ml^{-1}

In the counter the selected particle is directed into an optical chamber where a light source shines on it. The scattered light by the particle is focused to a photo detector where the intensity of the focused light is and indicator of the particle size as illustrated in the schematic diagram in figure 3.5. The counter is factory calibrated such that focused intensity implies a specific particle size

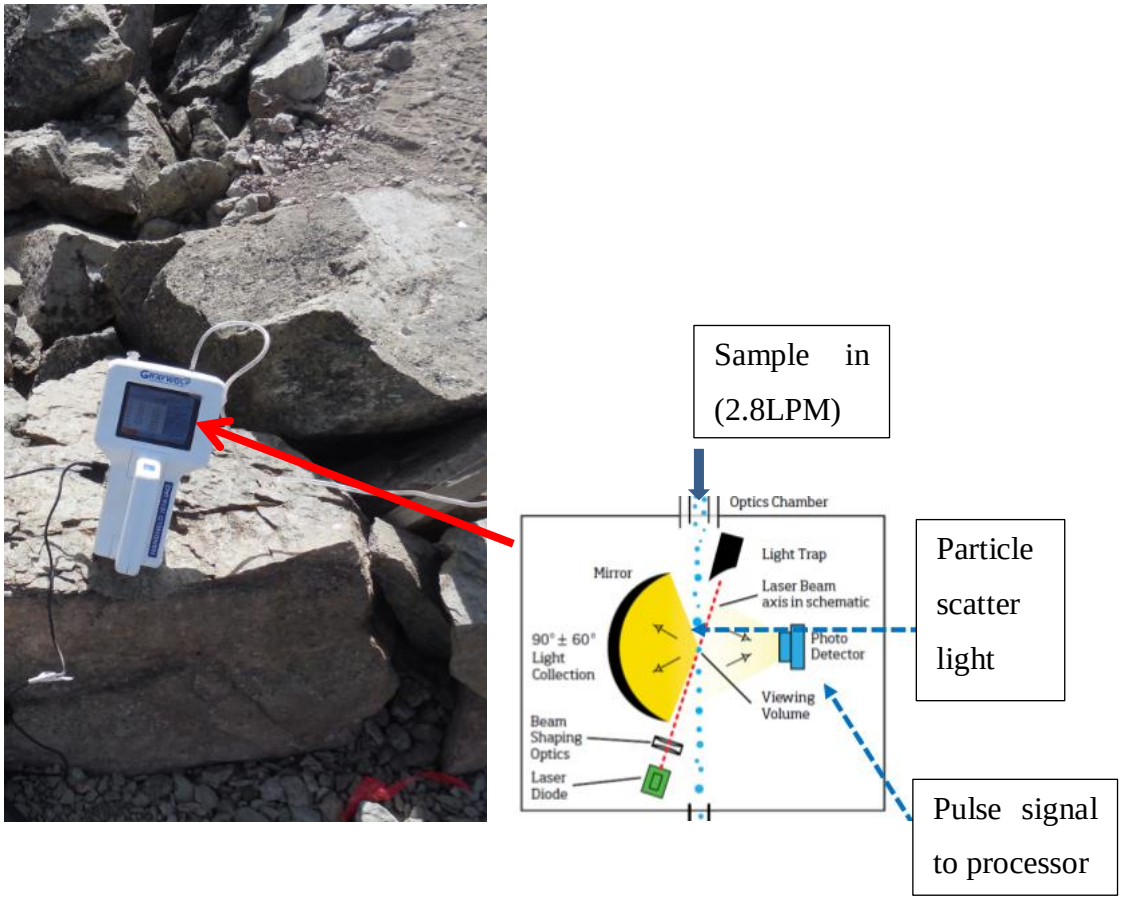

Figure 3.5: Particle counter and schematic diagram of its operation.

3.3.6 Wind speed

Seasonal monsoons are dominant in the tropical climatic region as the overhead sun crosses the equator resulting to Inter-Tropical Convergence Zone (ITCZ). Northeasterly

wind was observed. Speed of wind and direction was measures using a windmaster 2 anemometer (Kaindl) shown in Figure 3.6. Maximum and average wind speeds were recorded after every 8 h of sampling.

The anemometer had an inbuilt lithium battery which supplies power to the wind meter. A sensor head with bearing provides reading irrespective of the wind direction.

Figure 3.6: An anemometer indicating current, maximum and average wind speed in m s^{-1}.

3.4 Elemental Analyses

3.4.1. Filter analysis

The particulate matter collected on the filters was quantitatively analyzed for elemental content using an Energy Dispersive X-ray Fluorescence (EDXRF) spectrometer (shimanzu 800HS) at Material Testing and Research Laboratories in the Ministry of Transport, Infrastructure Housing and Urban Development .Figure 3.7 shows the spectrometer and a schematic presentation of its set up. The X-ray tube has Rh anode which is operated over a tube voltage range of 5 - 50 kV and a tube current of 1-1000 µA. The detector measured resolution was 140 eV for Mn-Kα at 5.9 keV.

Semiconductor Si(Li) detector mounted at 45^0 take off angle geometric with respect to the sample. The detector is cooled with liquid Nitrogen (LN_2) during measurements with approximate consumption of 1litre per day.

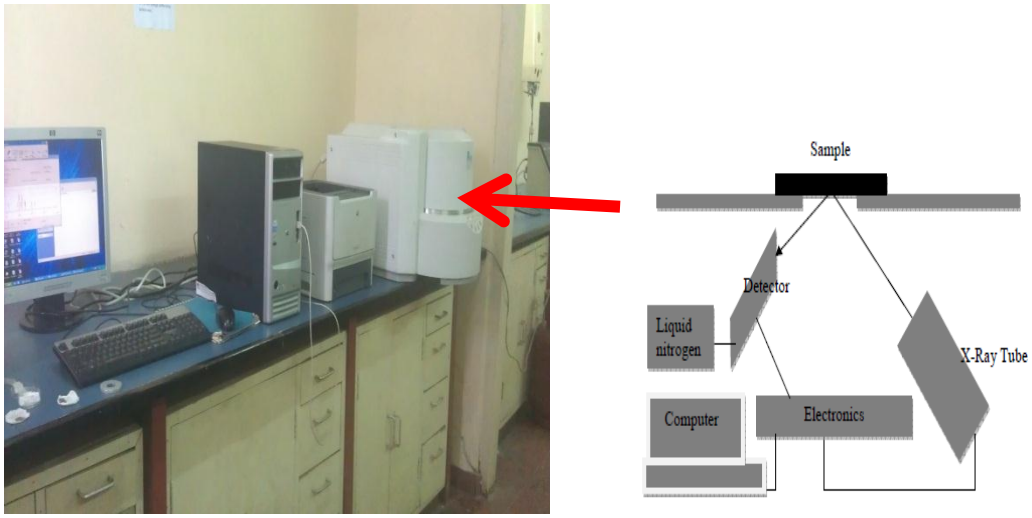

Figure 3.7: EDXRF (shimadzu-800HS) and schematic presentation of the instrumentation.)

The filters were irradiated for 1000 s and obtained spectra was processed for peak area determination. this was done using Analysis of X-ray spectrum by iterative least square (AXIL) software, which is a part of the software package, qaualitative x-ray analysis software (QXAS), supplied by international atomic energy agency (IAEA). The program enables elemental identification and quantification. Determining the detection limits ,the net peak areas of the elements of interest in the sample. Equation 3 is the formula used to calculate the limit of detection of the system.

$$DL = 3 \times C \times \frac{\sqrt{N_B}}{N_P} \quad \text{.....equation (3)}$$

where,

DL is the detection limit

C is the element concentration

N_p is the element's net peak area

N_B is the net background area under peak of the element

3.4.2 Glacier/water analysis

Samples from the glacier and water were analyzed in the laboratory using TXRF spectrometer (Bruker S2 picofox Benchtop TXRF spectrometer) shown in figure 3.8. This analytical method can be used to analyze elements from Na to U in the periodic table at concentrations ranging from 100% to sub-ppm. In a TXRF spectrometer the distance between the sample and the detector is kept small to increase detection efficiency of the fluorescence radiation. It is equipped with a Mo X-ray tube, and it is operated at 50 kV and 1000 µA, and detection limits of sub-µg L^{-1} are obtained.

Figure 3.8: TXRF (Bruker S2 picofox) at Institute of Nuclear Science and Technology and schematic presentation of the applied irradiation principles.

10 ml of the sample were pipetted into clean plastic vials where 10 µl of 1000 ppm Ga (element not present in the sample) was added as internal standard into the sample to make 1 ppm content in the vial. 10 µl drop of the content in the vial was transferred to the sample carrier which was then allowed to dry using a heating plate at 70ºC. The dried sample was then transferred to the TXRF spectrometer and analysed for 1000 sec at 50 kV and tube current of 1000 µA. Quantification was done using the S2 Picofox software provided by the manufacturer which uses the following formula (Equation 4):

$$\frac{N_x/S_x}{N_{is}/S_{is}} * C_{is} \ldots\ldots\ldots\ldots \text{equation (4)}$$

where,

C_x is the analyte concentration

C_{is} is the internal standard concentration

N_x is the analyte net intensity

N_{is} is the internal standard net intensity

S_x is the analyte relative sensitivity

S_{is} is the internal standard's relative sensitivity

3.4.3 Quality Control

The accuracy and validity of EDXRF method of analysis was determine using a sample of a standard reference material consisting of aerosol particles on a filter media, SRM 2783, from the National Institute of Standard and technology. To assess the effectiveness and reliability of TXRF procedure, resolution, sensitivity and intensity of the spectrometer were routinely determined before analysis of samples was done. Resolution was determined by analyzing 1 ng of Mn, sensitivity by analyzing 1 ng of Ni and intensity by analyzing 1 mg of As for count rate.

3.5 Data Analyses

Data management and presentation was done using Microsoft Excel spreadsheet and principal component analysis (PCA) was used for analysis. PCA analysis helps to identify patterns sources of the analysed species. The Scree Test is a program in PCA which helps in identifying main components of the highest percentage of explained variances.

CHAPTER FOUR

RESULTS AND DISCUSSION

4.1 Quality control

To ensure that the method of analysis by the EDXRF method was accurate and reproducible a sample of standard reference material consisting aerosols was analysed. The experimental and the certified values are presented in table 4.1. The elements of interest were within the range of the certified values.

Table 4.0.1: Measured and certified values of standard reference material (ng)

Elements	Detection Limits	Experimental Value	Certified Values	Recovery %
Ca	39	12680 ± 1200	13200 ± 1700	96
Ti	59	1606 ± 160	1490 ± 240	107
Cr	27	118 ± 17	135 ± 25	87
Mn	24	336±15	320 ± 12	105
Fe	43	26650 ± 1683	26500 ± 1600	101
Ni	12	72 ± 14	68 ± 12	106
Cu	18	398 ± 37	404 ± 42	99
Zn	40	1714 ± 126	1790 ± 130	96
Pb	22	222 ± 32	317 ±54	70

Recovery % = (mean measured value / mean certified value)*100

The quality control of the TXRF was done by running the standards ten times, and the mean and standard deviation were calculated (Table 4.2) .The standard samples for intensity, resolution and sensitivity which were analysed for 1000 s,100 s and 1000 s respectively.

Table 4.2: Measured intensity, sensitivity and resolution

Intensity (cts s^{-1})	sensitivity (cts µg s^{-1} mA^{-1})	resolution (eV)
32806	9.9	145.4
32225	9.8	146.2
32539	9.6	147.5
32027	9.3	145.7
32498	9.6	146.0
30976	9.2	147.2
36717	9.7	146.3
35468	9.5	147.1
35569	9.6	145.6
30616	9.7	147.5
33144	9.6	146.4
2058	0.2	0.8

4.2 Meteorological parameters

The sampling period covered five days and two nights for a duration of 8 hours daily. Temperature and Relative humidity were recorded every five minutes.

Northeasterly winds dominated with maximum and average wind speed at a range of 11 to 18 m s^{-1} and 2.8 to 4.3 respectively (Table 4.3). The mornings windy followed by calm afternoons and windy evenings hence the skewed daily average to low values. Lentini et al. (2011) Mt. Rwenzori reported an average annual wind speed of 3.58 m s^{-1}. There could a similarity which would be attributed to the fact that both are equatorial mountains hence might experience the same winds throughout the year.

Table 4.3: observed maximum and average wind speed

Date	Maximum (m s^{-1})	Average (m s^{-1})
03-02-15	13.9	4.2
03-03-15	11.1	3.1
03-04-15	12.5	2.8
03-05-15	18.3	4.3
03-06-15	14.4	3.2

Temperature was also recorded by both probes of the GrayWolf pack, and recorded values correlated with coefficient r^2 of 0.9 as shown in Figure 4.1 determined from linear regression. The obtained regression equation $y = 3.0x + 0.9$.

Temperature recorded by both probes was used independently. Probe TG 501 recorded an average of 1.9^{o}C and a range of -8.1^{o}C to 18.4^{o}C while IQ 610 had an average of 4.9 $^{\circ}$C and a range of -4.6^{o}C to 19.4^{o}C. Lentini et al., (2011) reported an annual average of -0.35 $^{\circ}$C.

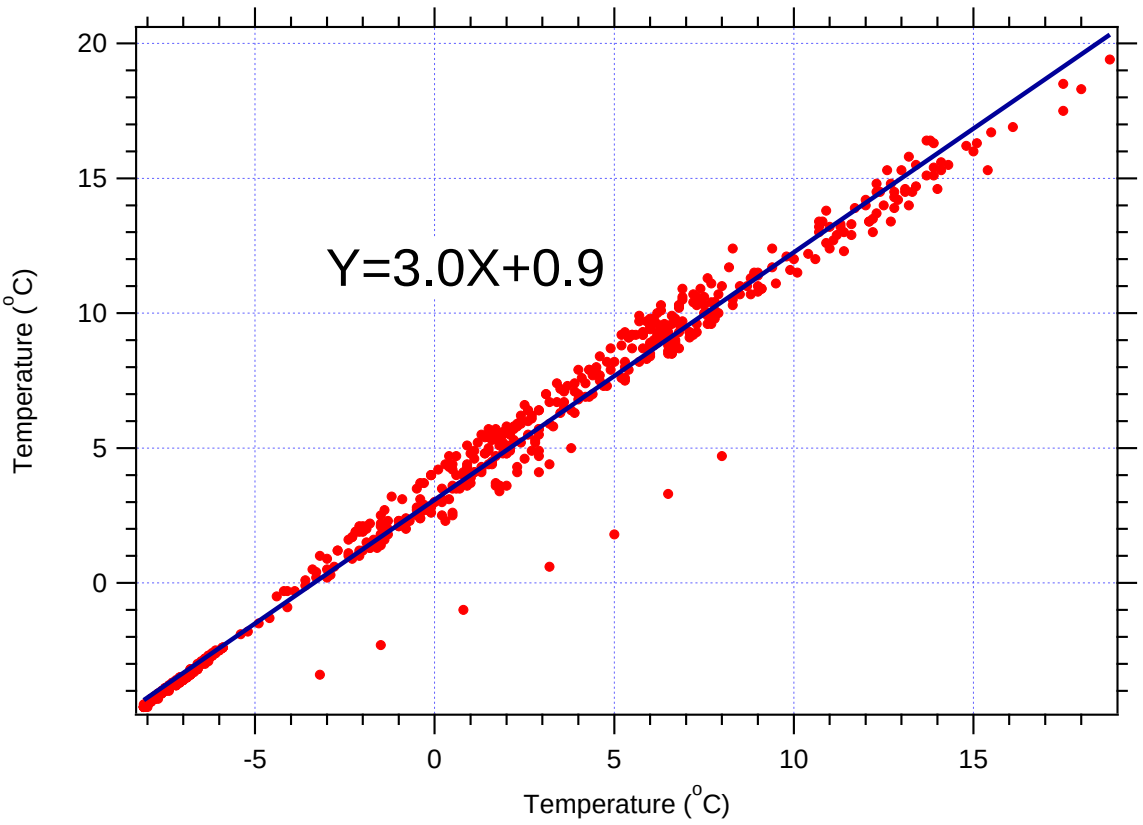

Figure 4.1 : Temperature recorded by probe IQ 610 versus that of probe TG 501.

Relative Humidity was low with no reported precipitation during the sampling period. This was expected given that it was during dry season of the year. Figure 4.2 shows mean percentage relative humidity for the morning and afternoon. Recorded range of RH was 10% to 64%. There afternoons were more humid than mornings.

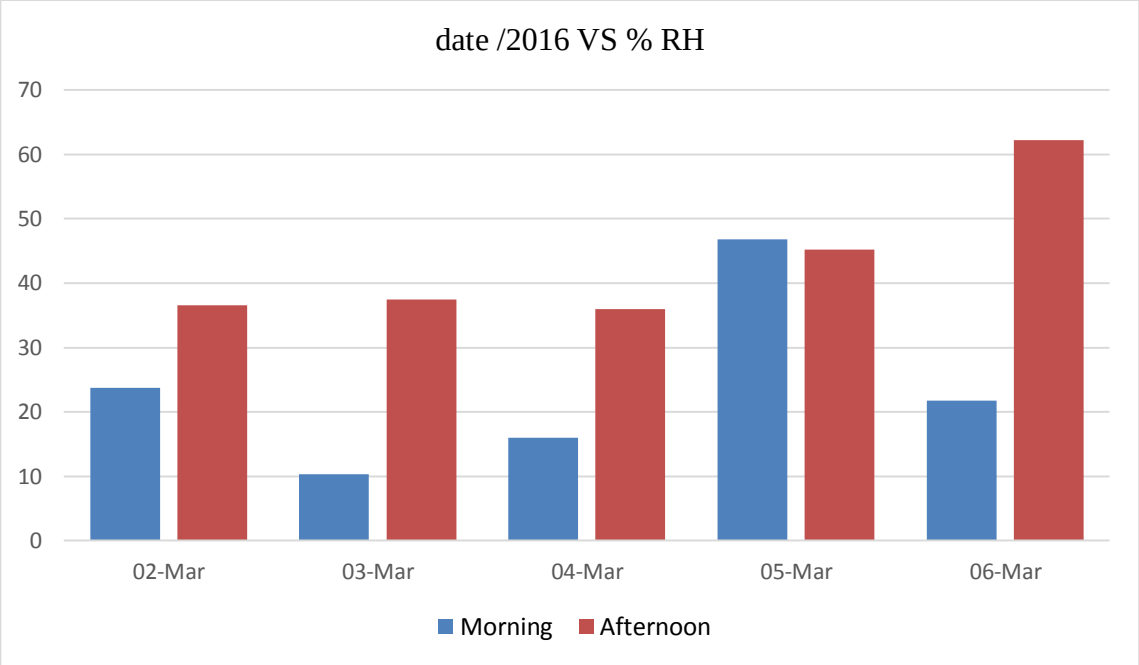

Figure 4.2: Morning and Afternoon mean Relative Humidity

4.2 Atmospheric concentration and Elemental composition of $PM_{2.5}$.

PM $_{2..5}$ in this study was observed in the range 11.8 - 148 ng m^{-3}, which was higher than reported by Gatari et al. (2009) from 3760 m altitude site on the same mountain but located at the northern western slopes. This suggested an increase in $PM_{2.5}$ emitting activities from 2001 to 2015..

The elemental composition of the sampled $PM_{2.5}$ was dominated by Ca at a range of 3.0 to 5.2 ng m^{-3} and Fe 0.9 to 1.0 ng m^{-3}, which were significantly higher than the other elements (Table 4.4*)*. These elements were 71-84% of the total elemental composition. This implied the main source of $PM_{2.5}$ were soils since these two elements are abundant in the earth's crust. However no significant difference was noted in elemental concentrations during the daytime and nighttime.

The concentration of most elements observed in this study were significantly lower than those reported by Gatari et al. (2009) in their study except Mn. Mn concentration range was 0.15 - 0.2 ng m^{-3}, which was lower than 0.7 - 2.8 ng m^{-3} reported by Gatari et al. (2009). This could be explained by the fact that their study was carried out at a lower

altitude than in this study thus suggesting dilution of the aerosol particles as attitude increased. It could also be as result of the fact that air density and pressure reduces with increase in attitude. Another reason could be the time of year when sampling was done hence differing of seasonal anthropogenic activities.

Table 4.4: Atmospheric concentration of the analyzed elements in $PM_{2.5}$ (ng m^{-3}).

	(Dates) /March 2015		
	02 – 03	04 – 05	05 – 06 (night)
$PM_{2.5}$	11.8 ± 2.8	148.9 ± 21.0	80.9 ± 19.7
Ca	3.0 ± 0.2	5.2 ± 2.3	4.2 ± 0.2
Ti	0.5 ± 0.1	0.7 ± 0.1	0.6 ± 0.1
Cr	0.2 ± 0.0	0.06 ± 0.01	0.10 ± 0.05
Mn	0.2 ± 0.1	0.15 ± 0.10	
Fe	1.0 ± 0.3	0.9 ± 0.2	1.0 ± 0.2
Ni	0.1 ± 0.0	0.07 ± 0.03	0.09 ± 0.04
Cu	0.3 ± 0.1	0.09 ± 0.02	0.20 ± 0.05
Zn	0.4 ± 0.1	0.23 ± 0.15	0.31 ± 0.12
Pb	0.1 ± 0.0	0.08 ± 0.02	0.10 ± 0.02

4.3 Particle Matter Counter

The instrument was set in the cumulative mode. Viewed data was the number of counts associated with each channel size is the number of particles that the instrument counted for that size and greater(Table 4.5).

Table 4.5 Observed cumulative Mean Daily PM counts

date	$PM_{0.3}$	$PM_{0.5}$	PM_{1}	$PM_{2.5}$	PM_{5}	PM_{10}	TPM
02-03-15	0	1.03	1.91	7.34	30.31	53.75	177.51
03-03-15	0	1.31	2.3	8.3	33.44	39.71	46.58
04-03-15	0	0.65	1.34	5.13	19.81	24.56	36.12
05-03-15	0	2.68	4.37	11.62	39.09	52.15	69.64
06-03-15	0	0.61	0.96	2.8	11.1	16.48	21.98
07-03-15	0	0.26	0.4	1.4	7.57	20.5	42.71

The observed data in figure 4.3 high daily mean counts of PM_5 ,PM_{10} and TPM than levels of $PM_{2.5}$ were reported but no $PM_{0.3}$. It implies that fine particles were less than Course particles hence there must have been very dusty due to the coarse dust particle.

Data collected was a clear indication that all the particles were as a result of a moving mass of air at any particular time of day. The particle counts would increase and decrease at the same time hence no new particle formation was taking place as indicated in the graph.

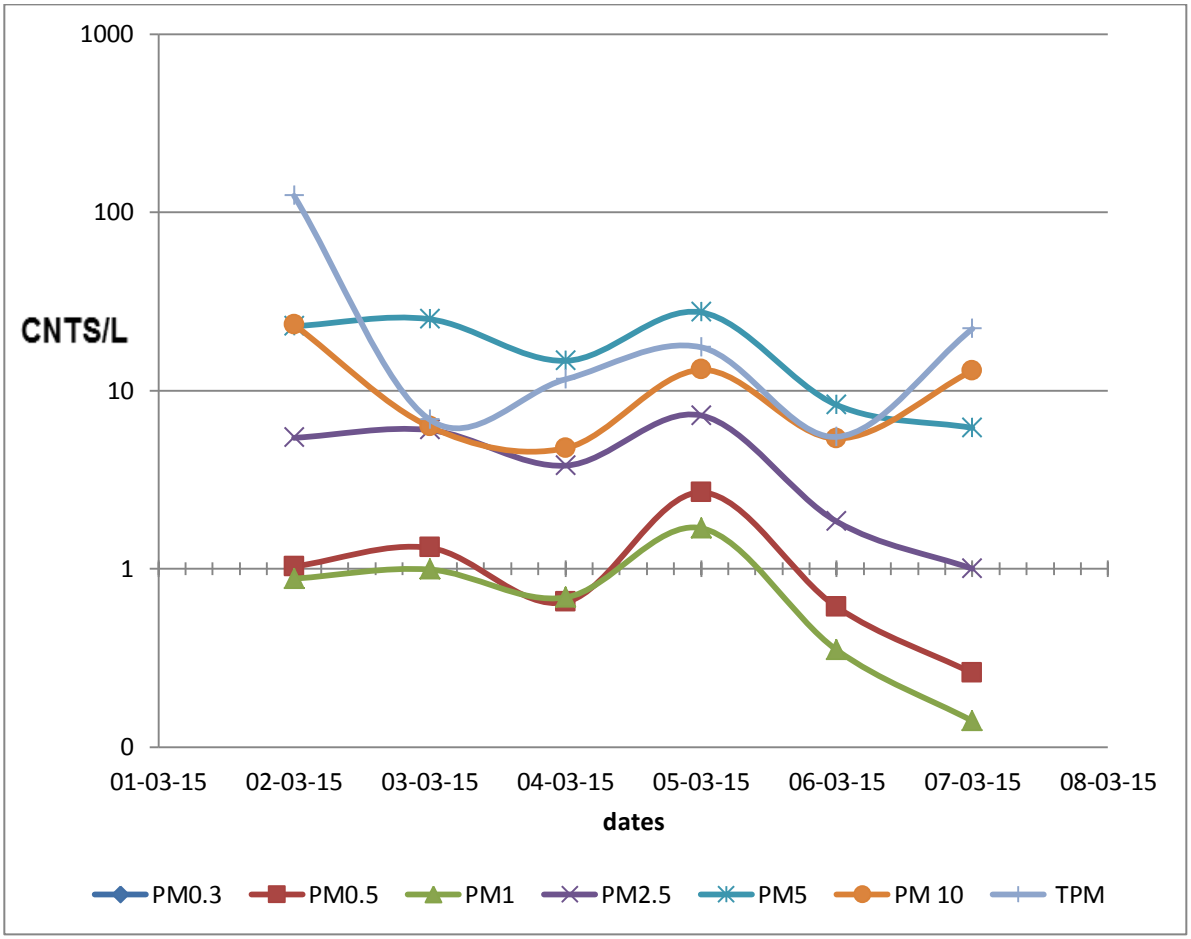

Figure 4.3: Daily mean counts of particles represented in each particulate mass(PM) fraction.

4.4 Black Carbon

Black carbon was recorded with the maximum concentration of 757 ng m^{-3} and a minimum of 78 ng m^{-3}. The mean was calculated from a treated data where negatives and the outliers were eliminated. However Gatari et al. (2009) reported higher values at 3678 m altitude on the same mountain ranging from 630 ± 110 ng m^{-3} to 2400 ± 430 ng m^{-3}. This variation could be as a result of decomposition and dilution of black carbon particles with the rises air (li et al., 2016).

Black carbon is associated with fine particulate matter. The BC sampler inlet had a $PM_{2.5}$ selective inlet and hence BC was sampled from $PM_{2.5}$. A plot of BC verses $PM_{2.5}$ counts sampled showed a linear correlation coefficient r^2 of 74% (Figure 4.4) .Although both variables were sampled using different instruments, it was evident that there is a relationship between $PM_{2.5}$ and BC concentration. In their study on Mt. Rwenzori, Robert et al. (2009) reported transportation of biomass burning products to East Africa from the horn of Africa by the north easterly winds. Li et al. (2016) reported the sources of Black carbon in Himalayas were from fossils fuels at 46 ± 11% and biomass combustion at 54 ± 11%.

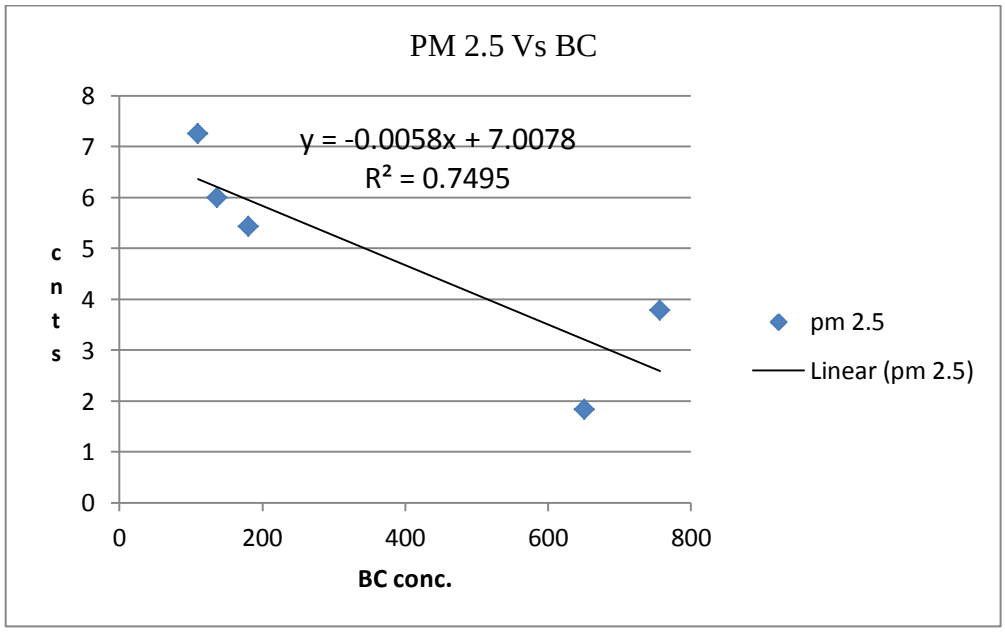

Figure 4.4: BC concentration versus $PM_{2.5}$ counts

4.4 Measurements of Atmospheric Gases

Nitrogen dioxide remained constantly low compared to Nitric Oxide which was evidently high with a the highest mean of 1162 ± 15.2µg m^{-3} on the 7th march 2015 and a low of 462.5 ± 328 µg m^{-3} on the 2nd march 2015. NO concentrations were also relatively high during the night while NO_2 remained constant (figure 4.5) for the sampling done for 8h daytime and night on the 5th and 6th March 2015. This would have been as a result of moving air mass rich in NO from far and surrounding regions. Lack of light that enhances the photolysis at night also might have attributed these high levels. . However due to limited data, this study could not establish the exact reason for this high concentration levels at night and day .

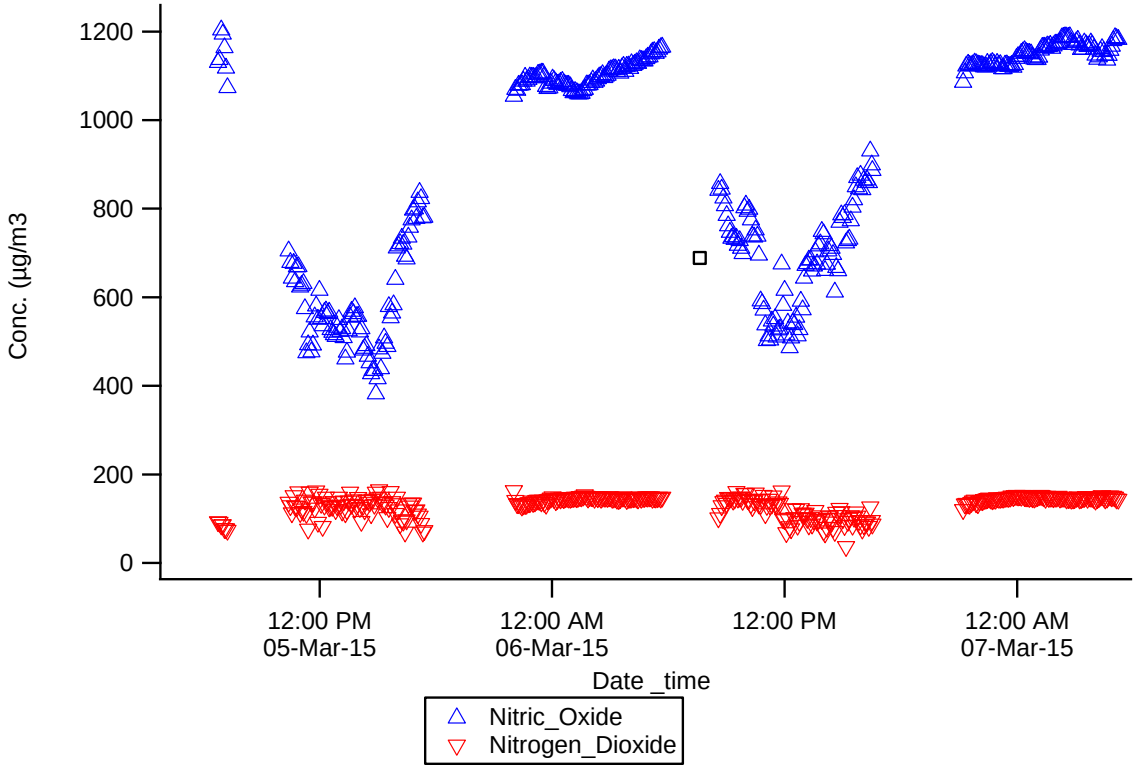

Figure 4.5 Nitric Oxide and Nitrogen Dioxide 8h day and night concentrations.

The most abundant gas that was observed was CO_2 with a maximum daily mean of 364 ± 53 mg m^{-3} over the measurement period. CO_2 have 0.38% abundance in air .Concentrations of CO_2, which implied high oxidation of their precursors, CO. NO was also relatively high throughout the study period suggesting continuous source contribution of these gases which could be natural or anthropogenic. (Figure 4.6 and appendix 1)

Observed concentration of TVOC was 330 ± 74 µg m^{-3}. No O_3 and SO_2 were observed during the sampling period. CO was only recorded on the first and second day of sampling with a mean of 9.9 ± 2 mg m^{-3}. However, these data was not used in this study because we could not account for irregularity of the data that could be as a result of faulty sensor or unaccountable environmental factors like nearby forest fires and charcoal burning.

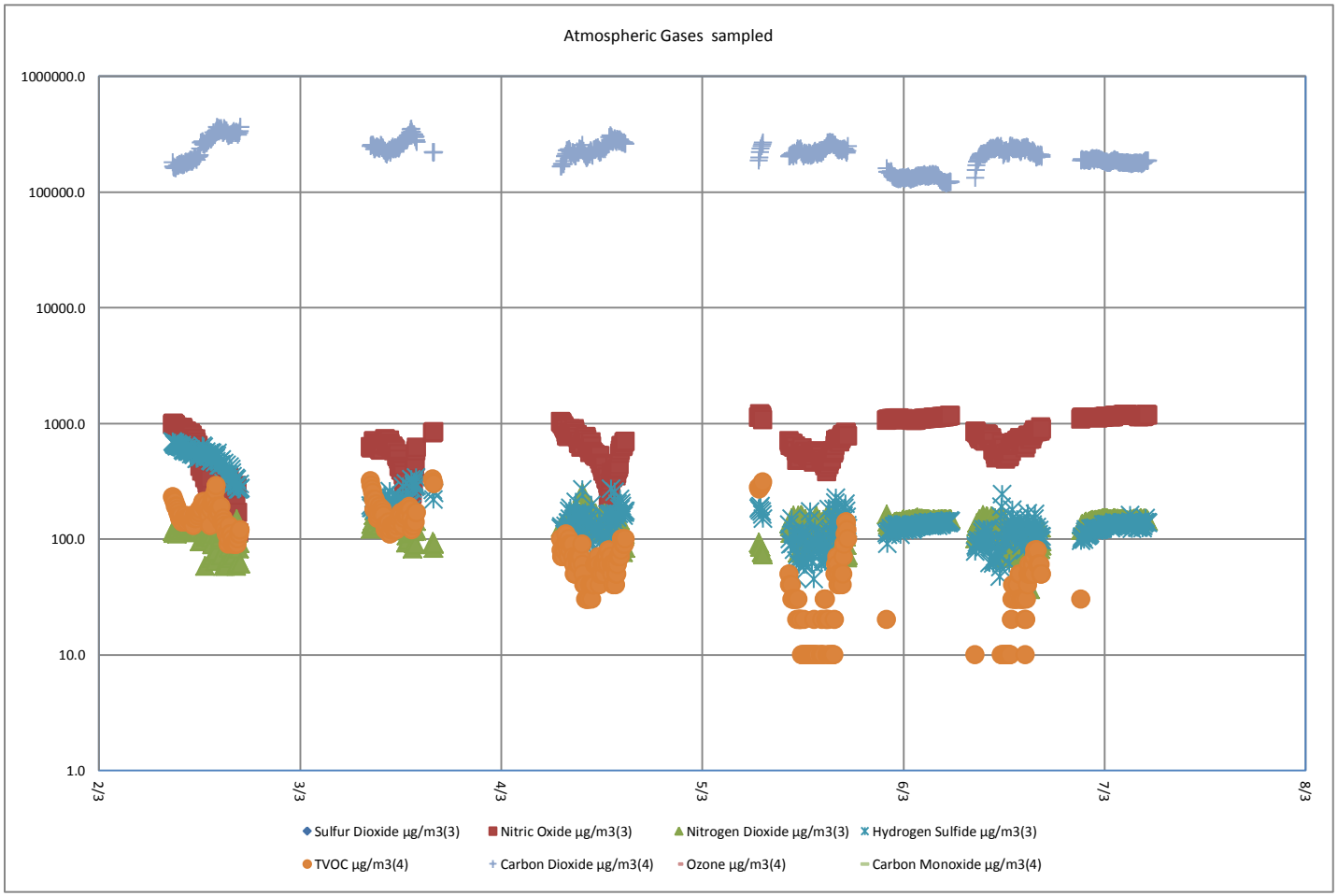

Figure 4.6. Sampled atmospheric gases and their concentrations

4.8 Elemental content of Glacier samples

It was observed that the concentrations of K, Ca, Ti, V, Mn, Fe, Cu and Br in the dirty glacier were significantly higher than those in the clean glacier as shown in (Table 4.7). This could suggest accumulation of pollutants resulting from anthropogenic activities and delivered to the site through the common convective system in the tropics and long-range transport. The amounts of Cr and Ni were relatively the same for both glaciers. Studies by Kaspari et al. (2009), Hong et al. (2009), Barbante et al. (2004) and Liu et al. (2011) reported an increase of trace elements in glaciers in the 20th century. They have also reported a reduction of some elements for instance Zn which is in agreement with this study where Zn was low in the clean glacier as compared to the dirty glacier. This was attributed to the lower emissions of those elements. However the levels of Ni and Cr in the melt water were higher than those found for the Glaciers. Nevertheless, the levels of most elements in dirty glacier were also higher than those in the raw water. Concentrations of elements in the raw water, were higher than those found in the clean glacier suggesting that the dissolved elements in the water were elevated by the pollutants from the glacier.

Table 4.6: Elemental content of the clean glacier, dirty glacier and raw water (µg l^{-1})

Element	Clean Glacier	Dirty Glacier	Raw Water
K	1867 ± 32	3427 ± 108	543.7 ± 39.3
Ca	517.4 ± 14.7	3912 ± 105	9791 ± 135
Ti	19.6 ± 3.3	43.3 ± 13.7	30.3 ± 0.1
V	6.0 ± 3.0	17.0 ± 7.5	13.0 ± 4.0
Cr	4.7 ± 2.0	5.0 ± 0.1	9.3 ± 3.1
Mn	22.6 ± 2.3	63.3 ± 8.0	8.8 ± 3.0
Fe	110.0 ± 4.3	742.0 ± 23.7	40.3 ± 4.0
Ni	BDL	4.33 ± 0.45	6.3 ± 2.0
Cu	6.8 ± 1.0	14.7 ± 3.0	8.0 ± 2.0
Zn	34.5 ± 1.3	28.5 ± 3.7	31.2 ± 3.0
Br	BDL	11.5 ± 1.70	BDL
Rb	BDL	7.2 ± 1.5	BDL
Sr	BDL	60.3 ± 3.7	20.5 ± 2.0

4.9 Possible elements sources

Using the PCA analysis, missing elements were replaced by the half values of their detection limits. Eigenvalues were generated for the Ca, Ti, Cr, Mn, Fe, Ni, Cu, Zn, and Pb to help in data reduction. The eigenvalues of the correlation matrix equals the variances extracted by the principal components. Only two principal components were considered to help in data extraction as indicated in the Scree plot (figure 4.7)

Figure 4.7: scree plot of Eigenvalues verses number of components

These PCA results indicates that most of the data information (variance of 90 %) was explained using only the first two principal components; PC1, 74% of the variance; PC2 accounted for 16%.

The component matrix (table 4.8) indicated Ca, Ti, Mn, Fe, Pb and Cu had positive value in both extracted PCA1. These elements would have been associated with mineral dust. PCA2 on the other hand, although weak accounting for only 16% Cr, Ni, Zn, Fe and Ti suggested these elements were mostly from industrial wastes

Table 4.7: Component Matrix by reduction extraction

	Component	
	1	2
ca	.967	.075
Ti	.978	.208
Cr	.965	-.262
Mn	.969	.096
Fe	.891	.445
Ni	.957	-.289
Cu	.945	.021
Zn	.978	-.199
PB	.993	-.063

This suggested that the possible anthropogenic sources of the zinc in the mineral dust were evident. Primarily Zn is released to soil from metal industrial wastes and use agricultural products like fertilizers and preservatives contain Zn and mining. As reported by Nriagu and Pacyna (1988) anthropogenic sources are responsible for an annual estimate of 1,193,000–3,294,000 metric tons of zinc released to soils.

Cu was also reported to have significantly high correlation, would be as a result copper mining activities in East African region especially Uganda. Mineral dust can be transported by the north-easterly winds originating from the horn of Africa towards the Equitor (Robert et al 2009; Lentini et al 2011).

Presence of Cr could also be linked to unsafe disposal of industrial wastes which may results to leakages into the land and water supply system. These may originates from metallurgical and refractory applications, pigments production, wood preservation, leather tanning and other anthropogenic uses that uses chromium as one the raw materials (Barnhart J. 1997)

CHAPTER FIVE

CONCLUSIONS AND RECOMEDATIONS

5.1 Conclusion

This study analyzed different parameters observed at Mt. Kenya (4800m a.s.l.) as a case study, and despite the logistic and environmental challenges, the study provided all the required information about $PM_{2.5}$ concentration and elemental composition, PM count rate, black carbon concentration and glacier elemental composition and the atmospheric gases.

It was evident that aerosol emission has really increased with time hence increase in deposition on the glacier that would explain the reduction of Mt. Kenya Glacier that has been witnessed in the last fifteen year.

For all the acquired parameters, it was more evident that all the aerosols and gases at that altitude are probably transported from afar distance through air movements and hence carrying along toxic gases from Motor vehicle in the surrounding towns and farms, burning of biomass, forest fire and human economic activities. PCA indicated that mineral dust containing Zn, Ca and Cu could have originated from a far distance not to mention the background emissions from the mountain itself being a dormant volcanic it might still be emitting some volcanic gases and elements. Therefore, this study implicated impact of long and short range transport which one would expect in the middle troposphere.

All these aerosols are transported on to the mountaintop's and are major causes of glacier degradation. Particles deposition on the glacier highly affect the albedo thus the earth end up retaining a lot of heat hence melting the snow as discussed by Marcq et al., (2010). Ambient aerosol particles plays a very important role in balancing the atmosphere not only by scattering and absorbing incoming and outgoing solar and terrestrial radiation but also modifying microphysical properties of clouds through cloud condensation nuclei (CNN) and ice Nuclei (IN).

5.2 Recommendation

It is evident from this study that the main sources of aerosols are mainly anthropogenic. This study can be used by policy makers to make informed decisions regarding mitigation of harmful aerosols emissions into the atmosphere that are transported to very far distances and to govern in decision making on climate change and high altitude pollution and reserve Mt. Kenya which is a very important water tower that supports Kenyan economy.

A similar study for a longer sampling period at the same altitude is recommended, possibly remotely and data sent via satellite due to the difficult terrain and logistics. However, short term studies and spaced in time over the year are necessary for validation of the data sampled remotely. This would avail more data to researchers, scientists and policy makers in regard to the state of mountain pollution and overall climate change.

References

Akhter, M. S., Chughtai, A. R., & Smith, D. M. (1985). The structure of hexane soot I: Spectroscopic studies. Applied Spectroscopy, 39(1), 154-167.

Andreae, M. O. (1990). Ocean - atmosphere interactions in the global biogeochemical sulfur cycle. Marine Chemistry, 30, 1-29.

Barbante, C., Schwikowski, M., Döring, T., Gäggeler, H. W., Schotterer, U., Tobler, L., Van, . V. K., Boutron, C. (2004). Historical Record of European Emissions of Heavy Metals to the Atmosphere Since the 1650s from Alpine Snow/Ice Cores Drilled near Monte Rosa. Environmental Science & Technology, 38(15), 4085-4090.

Barnhart , J. (1997) "occurrence , uses and properties of Chromium " regulatory toxicology and pharmacology 26, s3 –s7 RT 971132

BBC World news. (2015) Global warming 'doubles risk' of extreme weather. Retrieved on 6 February 2015 from; http://www.bbc.com/news/science-environment-30985039.

Bian, H. & Zender, C. S., (2003). Mineral dust and global tropospheric chemistry: Relative roles of photolysis and heterogeneous uptake, Journal of Geophysical Research, 108 (D21): 4672.

Bonasoni, P., Laj, P., Angelini, F., Arduini, J., Bonafe, U., Calzolari, F., Vuillermoz, E. Cristofanelli P, Decesari S, Facchini MC, Fuzzi S, Gobbi GP. (2008). The ABC-Pyramid Atmospheric Research Observatory in Himalaya for aerosol, ozone and halocarbon measurements. Science of the Total Environment, 391(2), 252-261.

Bonasoni, P., Laj, P., Marinoni, A., Sprenger, M., Angelini, F., Arduini, J., &Cristofanelli, P. (2010). Atmospheric Brown Clouds in the Himalayas: first two years of continuous observations at the Nepal-Climate Observatory at Pyramid (5079 m). Atmospheric Chemistry and Physics, 10(2), 4823-4885.

Bond T.C. & Sun H. L. (2005). Can reducing BC emissions counteract global warming? Environmental Science & Technology, 39: 16

Cai, J., Yan, B., Ross, J., Zhang, D., Kinney, P. L., Perzanowski, M. S., ... & Chillrud, S. N. (2014). Validation of MicroAeth® as a black carbon monitor for fixed-site measurement and optimization for personal exposure characterization. Aerosol and air quality research, 14(1), 1.

Cattell, R. B (1966) The Scree Test for the number of factors, Multivariate Behavioural Research, 1 (2) 245 – 276.

Flanner, M., Zender, C., Randerson, J., &Rasch, P. (2007). Present-day climate forcing and response from black carbon in snow. Journal of Geophysical Research: Atmospheres (1984–2012), 112 (D11).

Gatari M. J., Petterson J.,Kimani W., Boman J. (2009). Inorganic and black carbon aerosol concentrations at high altitude on Mt. Kenya.X-ray Spectrometer,38 (1): 26–36.

Haywood J. and Boucher O. (2000). Estimates of the direct and indirect radiative forcing due to tropospheric aerosols: A review. Reviews of Geophysics, 38 (4): 513.

Henne S., Klausen J., W. Junkermann W., Kariuki J. M., Aseyo J. O., Buchmann B. (2008) Representativeness and climatology of carbon monoxide and ozone at the global GAW station Mt. Kenya in equatorial Africa. Atmos. Chem. Phys., 8: 3119–3139.

Henne, S., Furger, M., Nyeki, S., Steinbacher, M., Neininger, B., De Wekker, S.,Prévôt, A. et al. (2004). Quantification of topographic venting of boundary layer air to the free troposphere. Atmospheric Chemistry and Physics,4(2), 497-509.

Hinds, W. C. (1999). Aerosol Technology: Properties, Behavior, and Measurement of airborne Particles 2nd ed. Newyork: John Wiley & Son Inc.s

Hong, Sungmin, Lee, Khanghyun, Hou, Shugui, Do Hur, Soon, Ren, Jiawen, Burn, Laurie J., Rosman, Kevin J. R., Boutron, Claude. (2009). An 800-Year Record of Atmospheric As,

Mo, Sn, and Sb in Central Asia in High-Altitude Ice Cores from Mt. Qomolangma (Everest), Himalayas. Environmental Science & Technology, 43(21) 8060-8065

Horvath, H. (1993). Atmospheric light absorption: A review. *Atmospheric Environment. Part A. General Topics*, 27(3), 293-317.

IPCC (2007). Climate change; Impact, adaptation and venerability. Fourth Assessment Report of the Intergovernmental Panel on Climate Change. Cambridge: Cambridge University Press..

IPCC (2013). Climate Change; The physical science basis. Fifth Assessment Report of the Intergovernmental Panel on Climate Change. Cambridge: Cambridge University Press..

Jacobson, M. Z. (2001). Strong radiative heating due to the mixing state of black carbon in atmospheric aerosols. Nature, 409(6821), 695-697.

Kahn, R., Gaitley, B., Garay, M., Diner, D., Eck, T., Smirnov, A. & Holben, B. (2010). Multiangle imaging spectro-radiometer global aerosol product assessment by comparison with the Aerosol Robotic Network. J. Geophys. Res., 115.

Kaser, G. (1999). A review of the modern fluctuations of tropical glaciers. Global and Planetary Change, 22(1), 93-103.

Kaser, G., Cogley, J., Dyurgerov, M., Meier, M., & Ohmura, A. (2006). Mass balance of glaciers and ice caps: consensus estimates for 1961–2004.Geophysical Research Letters, 33(19).

Kaspari, S., Mayewski, P. A., Handley, M., Osterberg, E., Sneed, S., Kang, S., Hou, S., Qin, D. (2009). Recent increases in atmospheric concentrations of Bi, U, Cs, S and Ca from a 350-year Mount Everest ice core record. Journal of Geophysical Research D: Atmospheres, 114,(4)

Kehrwald, N., Thompson, L., Tandong, Y., Mosley-Thompson, E., Schotterer, U., Alfimov, V. Davis, M. et al. (2008). Mass loss on Himalayan glacier endangers water resources. Geophysical Research Letters, 35(22).

Kite, G. W. (1982).Analysis of Lake Victoria levels. Hydrological Sciences Journal, 27(2), 99-110.

Lau, W. K., Kim, M., Kim, K., Woo-Seop (2010). Enhanced surface warming and accelerated snow melt in the Himalayas and Tibetan Plateau induced by absorbing aerosols, Envoronmental research letter 5: 2

Lentini G., Cristofanelli P., Duchi R., Marinoni A., Verza G., Vuillermoz E., Toffolon R., Bonasoni P., (2011). Mount Rwenzori (4750m a.s.l, Uganda): meteorological characterization and Air mass transport analysis. (IT ISSN 0391-9838, 2011).

Li, C., Bosch, C., Kang, S., Andersson, A., Chen, P., Zhang, Q., ... & Gustafsson, Ö. (2016). Sources of black carbon to the Himalayan–Tibetan Plateau glaciers. Nature Communications, 7, 12574.

Liu, Y., Hou, S., Hong, S., Hur, S. D., Lee, K., & Wang, Y. (June 27, 2011). High-resolution trace element records of an ice core from the eastern Tien Shan, central Asia, since 1953 AD. Journal of Geophysical Research: Atmospheres, 116.

Marcq, S., Laj, P., Roger, J. C., Villani, P., Sellegri, K., Bonasoni, P. Bergin, M.. (2010). Aerosol optical properties and radiative forcing in the high Himalaya based on measurements at the Nepal Climate Observatory-Pyramid site (5079 m asl). Atmospheric Chemistry and Physics, 10(13), 5859-5872.

Marinoni, A., Cristofanelli, P., Laj, P., Duchi, R., Calzolari, F., Decesari, S. Bonasoni, P.. (2010). Aerosol mass and black carbon concentrations, a two year record at NCO-P (5079 m, Southern Himalayas). Atmospheric Chemistry and Physics, 10(17), 8551-8562.

Masiello C. A. (2004). New directions in black carbon and organic geochemistry. Marine Chemistry, 92: 201– 213.

Ming, J., Xiao, C., Du, Z., & Yang, X. (2013). An overview of black carbon deposition in High Asia glaciers and its impacts on radiation balance. Advances in Water Resources, 55, 80-87.

Molg, t.,Rott, H., Kaser, G.,Fisher, A.,Cullen, N. (2006). Recent glacier recession in the Rwenzori mountains of East Africa due to rising air temperature. *Geophysical research letter*, 33.

NASA (1996). Atmospheric Aerosols: What Are They, and Why Are They So Important? Retrieved on February 2016 from;

http://www.nasa.gov/centers/langley/news/factsheets/Aerosols_prt.htm

Nriagu, J. O., & Pacyna, J. M. (1988). Quantitative assessment of worldwide contamination of air, water and soils by trace metals. nature, 333(6169), 134-139.

Ogren, J. A., & Charlson, R. J. (1983). Elemental carbon in the atmosphere: cycle and lifetime. Tellus B, *35*(4), 241-254.

Poschl U. (2005). Atmospheric Aerosols: Composition, Transformation, Climate and Health Effects. Angewandte Chemie, 44, 7520 – 7540.

Ramanathan V. and Carmichael G. (2008). Global and regional climate changes due to black carbon. Nature Geoscience, 1: 221-227

Ramanathan, V., Crutzen, P., Kiehl, J., & Rosenfeld, D. (2001). Aerosols, climate, and the hydrological cycle. Retrieved on August 2015 from;

http://www.sciencemag.org/cgi/content/full/294/5549/2119.

Ramanathan, V., Li, F., Ramana, M. V., Praveen, P. S., Kim, D., Corrigan, C. E. & Yoon, S. (2007). Atmospheric brown clouds: Hemispherical and regional variations in long-range transport, absorption, and radiative forcing. Journal of Geophysical Research: Atmospheres, (1984–2012), 112(D22).

Roberts, G., Wooster, M. J., & Lagoudakis, E. (2009). Annual and diurnal african biomass burning temporal dynamics. Biogeosciences, 6(5).

Seinfeld J. & Pandis S. (1998). Atmospheric Chemistry and Physics: From Air Pollution to Climate Change (2nd ed.), (p. 97). Hoboken, New Jersey; John Wiley & Sons, Inc..

Shaltout, A., Boman, J., Al-Malawi, D., Shehadeh, Z. (2013). Elemental composition of PM2.5 particles sampled in industrial and residential areas of Taif, Saudi Arabia. Aerosol and Air Quality Research, 13: 1356 – 1364, 2013.

Taylor, R., Mileham, L., Tindimugaya, C., Majugu, A., Muwanga, A., &Nakileza, B. (2006). Recent glacial recession in the Rwenzori Mountains of East Africa due to rising air temperature. Geophysical Research Letters, 33(10).

Twomey S. (1977). The influence of pollution on the shortwave albedo of clouds.Journal of the Atmospheric Sciences,34 (7): 1149–1152.

UNEP/GRID-Arendal. Shrinking Lewis Glacier, Mount Kenya [Internet]. UNEP/GRID-Arendal Maps and Graphics Library; June 2007. Retrieved on November 2016

http://maps.grida.no/go/graphic/shrinking-lewis-glaciermount-kenya

Voiland, A and Simmon, R. (2010). Aerosols: tiny particles, big impact.Retrieved on February 2016 from

http://earth observatory.nasa.gov/Features/Aerosols/

Wada, M., Tsukada, M., Namiki, N., Szymanski, W. W., Noda, N., Makino, H., Kamiya, H. (2016). A Two-Stage Virtual Impactor for In-Stack Sampling of PM2. 5 and PM10 in Flue Gas of Stationary Sources. Aerosol and Air Quality Research, 16(1), 36-45.

Xu, B., Cao, J., Hansen, J., Yao, T., Joswia, D. R., Wang, N. He, J. et al., (2009). Black soot and the survival of Tibetan glaciers. Proceedings of the National Academy of Sciences, 106(52), 22114-22118.

Yao, T., Wang, Y., Liu, S., Pu, J., Shen, Y., & Lu, A. (2004). Recent glacial retreat in High Asia in China and its impact on water resource in Northwest China. Science in China Series D: Earth Sciences, 47(12), 1065-1075.

Yasunari, T. J., Bonasoni, P., Laj, P., Fujita, K., Vuillermoz, E., Marinoni, A.& Lau, K. M. (2010). Estimated impact of black carbon deposition during pre-monsoon season from Nepal Climate Observatory–Pyramid data and snow albedo changes over Himalayan glaciers. Atmospheric Chemistry and Physics, 10(14), 6603-6615.

Yu, H., Kaufman, Y., Chin, M., Feingold, G., Remer,L., Anderson, T., Balkanski,Y. et al. (2006). A review of measurement based assessments of the aerosol direct radiative effect and forcing, Atmospheric Chemistry and Physics, 6, 613 – 666.

Appendix 1: Daily mean atmospheric gases (µg m^{-3}) of the sampled gases

Date	NO	NO_2	NH_4	H_2S	Temp-1(ºC)	TVOC	CO_2	O_3	Temp-2(ºC)	RH
2-Mar-15	462.3	114.4	18.3	504	9.1	158.6	259622	0	6.6	31.3
3-Mar-15	526.8	139.5	26.1	215.6	9.1	167.1	258414	0	6.1	20.8
4-Mar-15	612.3	136.6	36	144.1	6.6	63.6	236967	0	3.9	23.8
5-Mar-15	723.5	126.3	30.7	116.9	4.8	38.7	210500	0	1.8	38.9
6-Mar-15	910.8	130.2	49	118.5	0.5	11	187015	0	-2.7	30.8
7-Mar-15	1162.9	147.9	0	134.8	-4.2	0	181312	0	-7.7	18
Max	1162.9	147.9	49	504	9.1	167.1	259622	0	6.6	38.9
Min	462.3	114.4	0	116.9	-4.2	0	181312	0	-7.7	18
Average	733.1	132.5	26.68	205.7	4.32	73.17	222305	0.00	1.33	27.27

Appendix 2: Filter Data

	filters wt. before sampling			after sampling		
filter code	wt1	wt2	wt3	Wt1	Wt2`	Wt3
FEB 148	94.4	94.4	94.5	94.8	94.8	94.8
FEB 149	95.7	95.5	95.4	95.9	96	96
FEB 150	93.5	93.6	93.5	94.3	94.3	94.3
FEB 145	93.7	93.7	93.8	94.1	94	94
FEB 107	93.4	93.2	93.4	93.7	93.5	93.6
FEB 108	98.3	98.2	98.2	98.5	98.6	98.5
FEB 103	94.4	94.4	94.5	94.7	74.7	94.7
FEB 104	96.6	96.5	96.5	97	96.9	96.9
FEB 105	96.4	96.4	96.2	96.3	96.3	96.3
FEB 109	98.5	98.5	98.3	98.7	98.5	98.5
FEB 110	100.6	100.4	100.5	100.6	100.6	100.5
FEB 143	98.8	99.1	98.7	99.3	99.3	99.3
FEB 144	99.8	99.9	99.8	99.8	100	99.8
FEB 141	99.2	99	99.2	99.2	99.3	98.9
FEB 142	100.2	100.4	100.4	100.3	100.3	100.2

filter no.	Ca	Ti	Cr	Mn	Fe	Ni	Cu	Zn	Pb
149	9282.463	1279.465	403.8343	729.2583	3657.71	500.571	1241.272	1458.556	312.794
150	9201.336	1441.826	427.4225	700.988	3566.687	476.492	1156.319	1392.619	323.59
145	8265.974					27.867	643.5665	284.937	
107	8571.437			103.9895	976.9465	67.4975	287.354		
108	11700	851.2695		198.9935	3679.481		178.389		288.817
103	9604.889	400.208		96.779	820.1937		146.999		130.6263
104	26626.67	4129.443	174.6333	855.6857	3.722333		153.2757	495.043	259.0397
105	5854.54	1180.609	194.5737	417.0697	8124.499	209.0663	650.3613	1183.889	
109	16860	3578.664	191.5425	604.008	2.765		157.3155	346.4735	278.0855
110	10184.33	1257.016	194.567	377.672	4996.397	213.395	477.565	765.5275	206.5425
141	9402.434	820.52	404.577	300.0607	1721.242	474.092	474.4773	1300.437	252.7877
142	8720.903	607.038		99.286	748.4885		92.4255		166.0655
144	9827.672	1521.782	444.4575	756.1675	4226.748	493.7535	1313.988	1413.177	296.616

Appendix 3 : Hourly mean sampled gases, temperature and Relative humidity

	Sulfur Dioxide µg/m3(3)	Nitric Oxide µg/m3(3)	Nitrogen Dioxide µg/m3(3)	Ammonia µg/m3(3)	Hydrogen Sulfide µg/m3(3)	Temperature °C(3)	TVOC mg/m3(4)	Carbon Dioxide mg/m3(4)	Ozone µg/m3(4)	Carbon Monoxide µg/m3(4)	Temperature °C(4)	Relative Humidity %RH(4)
02-03-15												
8-9 am	0.2	945.4	125.1	0.0	660.1	0.8	0.2	168.5	0.0	7951.0	-3.1	22.3
9-10am	0.0	864.9	134.6	0.0	604.5	3.3	0.1	177.5	0.0	6446.2	-0.8	22.8
10-11am	2.233333	176.7467	94.26267	49.24667	314.5907	10.31333	0.1	327	0	109.96	8.12	43.04667
11-12pm	2.390909	211.8364	101.4855	33.83636	368.2709	10.77273	0.120909	327.6364	0	250.3182	8.918182	40.88182
12-1pm	12.55	77.25833	110.1833	20.15833	479.8408	15.45	0.1975	343.8333	0	2375.108	14.40833	33
1-2pm	1.566667	250.2083	103.0658	29.85	525.9175	14.64167	0.1875	288.1667	0	3860.733	13.60833	32.6
2-3pm	0.441667	471.475	116.0175	6.8	555.1508	11.11667	0.184167	242.5	0	4762.917	8.875	27.85
3-4pm	0.516667	751.0667	134.6767	0	559.87	6.1	0.149167	190.6667	0	5092.892	2.141667	25.825
03-03-15												
8-9 am	0	643.45	150.3433	0	197.5342	5.425	0.22	246.3333	0	6165.675	1.691667	7.975
9-10am	0	653.7917	159.3942	0	205.89	6.4	0.1575	234.3333	0	2672.35	2.958333	10.175
10-11am	0	634.6833	154.5683	0	200.4975	7.875	0.125	233.0833	0	1279.983	4.666667	12.225
11-12pm	0	452.7	140.7908	0	194.945	12.90833	0.145	253.6667	0	547.45	10.625	12.675
12-1pm	0	226.7	117.192	0.01	217.408	15.62	0.17	303.3	0	158.16	13.32	20.88
1-2pm	0.075	499.6583	110.8133	152.4	277.915	7.566667	0.185833	287.25	0	0	4.316667	61.04167
04-03-15												
7-8 am	0	907.1667	132.3733	0	124.9467	0.341667	0.0825	196.8333	0	0.55	-2.95833	10.49167
8-9am	0.036364	834.1909	153.4045	0	160.8345	2.136364	0.072727	216.6364	0	0	-1.83636	14.35455
9-10am	0	690.27	167.999	0	152.336	4.93	0.064	228.8	0	0	1.07	16.88
10-11am	0.0	667.6	153.9	0.0	136.1	6.2	0.0	210.9	0.0	0.0	3.5	20.8
11.12pm	0.0	621.0	144.1	15.2	186.8	6.9	0.1	241.1	0.0	1082.4	3.7	18.7
1-2pm	0	361.9		64.22727	166.33	9.645455	0.055455	287.1818	0	0	7.563636	34.6

				114.5418									
2-3pm		0	572.9182	107.6036	212.8909	184.7309	5.463636	0.080909	273.7273	0	0	3.409091	57.95455
	05-05-15												
6-7am		0	1089.925	83.43125	45.3125	175.5063	0.925	0.26375	236	0	1.25	2.5625	36.775
10-11am		0	658.5	131.4778	22.76667	108.7411	5.2	0.035556	210.6667	0	0	1.6	52.1
11-12pm		0	542.5545	128.5136	3.463636	86.05818	8.227273	0.021818	226	0	0	4.936364	42.55455
12-1pm		0.008333	542.5333	129.1992	0.016667	93.7225	9.8	0.010833	212.9167	0	0	6.266667	36.39167
1-2pm		0	533.275	132.935	0	88.14417	10.21667	0.008333	217.25	0	0	6.766667	33.575
2-3pm		0	464.1455	130.4618	0	80.68091	10.47273	0.017273	231.4545	0	0	6.945455	30.9
2-3pm		0.161538	533.7308	137.3631	31.02308	145.8646	6.338462	0.016923	262.0769	0	0	3.692308	42.58462
4-5pm		0	761.7353	104.8524	165.5294	148.0335	2.876471	0.074118	233.0588	0	0	-0.16471	71
10-11 pm		0	1082.375	136.5392	0	116.51	-2.95	0.001667	146	0	0	-6.425	16.125
11-12am		0	1092.775	139.9533	0	126.7133	-2.98333	0	131.8333	0	0	-6.50833	17.425
12-1am		0	1083.075	145.63	0	126.3142	-2.76667	0	132.6667	0	0	-6.31667	15.075
1-2am		0	1067.525	149.0817	0	127.1975	-2.51667	0	134.6667	0	0	-6.025	13.68333
2-3am		0	1095.758	148.2108	0	134.7458	-3.075	0	138.5833	0	0	-6.55	14.79167
3-4am		0	1115.233	146.0683	0	135.6367	-3.44167	0	140	0	0	-6.89167	14.75
4-5am		0	1129	146.881	0	136.771	-3.57	0	130.1	0	0	-7.11	16.69
5-6am		0	1152.309	147.7273	0	141.04	-3.96364	0	121.6364	0	0	-7.54545	19.03636
	06-03-15												
8-9am		0	788.1182	134.9482	0	92.34273	0.872727	0.000909	188.2727	0	0	-2.56364	16.83636
9-10am		0	749.0875	150.1875	0	106.7938	2.45	0	217.625	0	0	-0.3875	21.175
10-11am		0	683.6727	137.9	0	82.72727	4.690909	0	235.5455	0	0	2.7	20.08182
11-12pm		0	549.2833	132.1525	17.14167	109.4008	8.45	0.0025	237.4167	0	0	5.375	28.16667
12-1pm		0	544.5417	99.69833	128.3	115.5717	8.9	0.0125	230.5833	0	0	6.1	43.88333
1-2pm		0	696.2333	97.70333	182.8917	123.455	4.091667	0.035833	235.4167	0	0	1.183333	60.6
2-3pm		0	703.2833	96.23083	174.5	110.1867	4.208333	0.031667	236.5833	0	0	1.391667	61.05833
3-4pm		0	804.1167	90.72	210.95	124.8142	2.608333	0.064167	216.25	0	0	-0.425	76.21667
4-5pm		0	880.6	94.72	170.4857	105.9157	1.3	0.055714	207.5714	0	0	-1.81429	74.28571

9-10pm	0	1119.37	134.092	0	106.716	-3.56	0.003	189.8	0	0	-6.99	26.63
10-11pm	0	1124.717	143.3133	0	118.2108	-3.55	0	191.25	0	0	-7.04167	20.75
11-12am	0	1123.558	148.5517	0	124.29	-3.50833	0	190.5833	0	0	-6.98333	18.95833
12-1am	0	1147.667	149.3717	0	131.6942	-3.9	0	181.9167	0	0	-7.41667	19.90833
1-2am	0	1161.225	149.1325	0	134.9442	-4.2	0	185.5833	0	0	-7.675	19.075
2-3am	0	1180.025	146.4283	0	136.5008	-4.48333	0	179.75	0	0	-7.98333	18.56667
3-4am	0	1169.183	147.145	0	135.4025	-4.21667	0	177.3333	0	0	-7.75833	16.65
4-5am	0	1159.047	147.3967	0	135.4167	-4.08	0	181.6	0	0	-7.62	16.25333